Multiresolution Representations using the Auto-Correlation Functions of Compactly Supported Wavelets

Naoki Saito*
Schlumberger–Doll Research
Old Quarry Road, Ridgefield, CT 06877-4108

Gregory Beylkin
Program in Applied Mathematics
University of Colorado at Boulder, Boulder, CO 80309-0526

August 15, 1991
Revised January 9, 1992
Submitted to the special issue of IEEE Transactions on Signal Processing on Wavelets and Signal Processing

Abstract

In this paper we propose a "hybrid" shift-invariant multiresolution representation which utilizes dilations and translations of the auto-correlation functions of compactly supported wavelets. In this representation, the exact filters for the decomposition are the auto-correlation of the quadrature mirror filter coefficients of the compactly supported wavelets. The decomposition filters are, therefore, exactly symmetric. Moreover, the auto-correlation functions of the compactly supported wavelets may be viewed as pseudo-differential operators of the even order and behave, essentially, as the derivative operators of the same order. This allows us to relate the zero-crossings in this representation to the locations of edges at different scales in the signal. The recursive definition of the compactly supported wavelets and, therefore, their auto-correlation functions, allows us to construct fast recursive algorithms to generate the multiresolution representations. Though it is not an orthogonal representation, there is a simple relation with the wavelet-based orthogonal representations on each scale. We describe a simple reconstruction algorithm to recover functions from such expansions.

A remarkable feature of the representation using the auto-correlation function of compactly supported wavelets is a natural interpolation algorithm associated with it. This interpolation algorithm, the so-called symmetric iterative interpolation, is due to Dubuc [1] and Deslauriers and Dubuc [2]. The coefficients of the interpolation scheme of [1] and [2] generated from the Lagrange polynomials are the auto-correlation coefficients of quadrature mirror filters associated with the compactly supported wavelets of Daubechies.

*Also with Department of Mathematics, Yale University, New Haven, CT 06520

Finally, we consider the reconstruction of signals from zero-crossings (and slopes at zero-crossings) of their multiresolution representations. Our approach permits a non-iterative reconstruction from zero-crossings (and slopes at zero-crossings). Using the interpolation algorithm mentioned above, we locate the zero-crossings and compute slopes at these points within the prescribed numerical accuracy. We then set up a linear system, where the entries of the matrix are computed from the values of the auto-correlation function and its derivative at the integer translates of zero-crossings. The original signal is reconstructed within the prescribed accuracy by solving this linear system.

I Introduction

The information about the local behavior of a function is hidden in the decay (or growth) from scale to scale of the coefficients of the orthonormal wavelet expansions (see e.g. Chapter VI of [3]). Exploiting this property in applications, however, is not a straightforward exercise due to the fact that the coefficients of the orthonormal wavelet expansions are not shift invariant. In implementing multiresolution algorithms for image processing and signal analysis, redundant representations are being used in order to simplify the analysis of coefficients from scale to scale (see e.g. [4]).

Another difficulty in utilizing the orthonormal wavelets for the analysis of signals in image processing is associated with the asymmetric shape of compactly supported wavelets [5]. On the one hand, using compactly supported wavelets implies that the associated exact quadrature mirror filters are of finite size and, therefore, are exact in computer implementations. On the other hand, the symmetric basis functions are preferred in image processing since their use simplifies finding zero-crossings (or extrema) corresponding to the locations of edges in images at later stages of processing. There are two approaches for dealing with this problem. The first approach consists in constructing approximately symmetric orthonormal wavelets and gives rise to approximate quadrature mirror filters [6]. The second consists in using biorthogonal bases [7], [8], so that the basis functions may be chosen to be exactly symmetric. In fact, a modified Laplacian pyramid of Burt and Adelson may be reinterpreted as a biorthogonal decomposition [7].

In this paper, we propose a "hybrid" multiresolution representation which utilizes dilations and translations of the auto-correlation functions of compactly supported wavelets. In this representation, the exact filters for the decomposition (similar to the quadrature mirror filters) are symmetric. The auto-correlation functions of the compactly supported wavelets may be viewed as pseudo-differential operators of even order and behave, essentially, as derivative operators of the same order. This allows us to relate the zero-crossings in this representation to the locations of edges at different scales in the signal. The recursive definition of compactly supported wavelets and, therefore, of their auto-correlation functions, allows us to construct fast recursive algorithms to generate the multiresolution representations. Though it is not an orthogonal representation, there is a simple relation with the wavelet-based orthogonal representations on each scale. We describe a simple reconstruction algorithm to recover functions from such expansions.

A remarkable feature of the representation using the auto-correlation function of the compactly supported wavelets is a natural interpolation algorithm associated with it. This interpolation algorithm, the so-called symmetric iterative interpolation, is due to Dubuc [1] and Deslauriers and Dubuc [2]. The coefficients of the interpolation scheme of [1] and [2] generated from the Lagrange polynomials are the auto-correlation coefficients of the quadrature mirror filters associated with the compactly supported wavelets of [5]. This connection was also noticed by Shensa in [9]. This interpolation scheme of Dubuc is also related to the "algorithme à trous" in [10], [11].

Finally, we consider the reconstruction of signals from zero-crossings (and slopes at zero-crossings) of their multiresolution representations. There is a long history of research on reconstructing signals from their zero-crossings in the multiresolution representations of the signal. (We refer to Hurt [12] for other representations.) The problem of reconstructing signals from their zero-crossings in the multiresolution representation arises in image processing in modeling of the visual systems of mammals (see D. Marr [13]). The question is whether it is possible to reconstruct the

original signal (image) from its multiresolution edges which correspond to the zero-crossings in the multiresolution representation of the signal. Marr used convolutions of the signal with the second derivative (Laplacian) of a Gaussian distribution to generate the multiresolution representation. The scale parameter in this case is the standard deviation σ of the Gaussian. Witkin [14] considered the continuous scale parameter and proposed the signal description in the "scale space". By considering the original signal as an initial temperature distribution, Koenderink [15] interpreted this scale-space representation as an evolution of the solution of the heat equation. Using the maximum principle for the heat equation, Yuille and Poggio [16], [17], and Hummel and Moniot [18], [19] showed that if the original signal(1-D) is a polynomial, then the reconstruction from its zero-crossings is theoretically possible. However, the stability of the reconstruction cannot be guaranteed through their approach. Hummel and Moniot empirically stabilized the reconstruction by using the slopes at the zero-crossings but did not prove the convergence and the stability of the reconstruction.

S. Mallat [20] proposed a new reconstruction method based on the wavelet representation. This method uses zero-crossings and integral values of signals (or signal energies) between the adjacent zero-crossings in a redundant wavelet representation. Using the alternating projections (the so-called "projection onto convex sets"), Mallat proposed an iterative algorithm for reconstructing the signal. Mallat and S. Zhong [21] used the maxima and their magnitudes in the redundant wavelet representation instead of the zero-crossings. This approach leads to iterative, empirically convergent algorithms but there is no proof of the uniqueness of the reconstruction.

Our approach does not rely on the continuous scale parameter, which was necessary for the heat equation formalism, neither does it use the iterative projection algorithm. Instead, we use the dilations and translations of the auto-correlation functions of compactly supported wavelets to derive a non-iterative reconstruction algorithm in Section V. Using the interpolation algorithm mentioned above, we locate the zero-crossings and compute slopes at these points with prescribed numerical accuracy. We then set up a linear system, where the entries of the matrix are computed from the values of the auto-correlation function and its derivative at the integer translates of zero-crossings. This matrix is always sparse because of the compact supports of these auto-correlation functions. The original signal is reconstructed within the prescribed accuracy by solving this linear system.

Our results can also be viewed as a way to obtain the continuous-like multiresolution analysis starting from the discrete multiresolution analysis. Another approach to make the connection between continuous and discrete multiresolution analyses is developed by Duval-Destin et al. [22], where the starting point is the continuous version of the multiresolution analysis.

The organization of this paper is as follows. In Section II we introduce the notion of the *orthonormal shell* expansion of signals which generates a shift-invariant representation using the orthonormal wavelets. In Section III we consider expansion of signals into the *auto-correlation shell*, i.e., expansion into a family of functions consisting of dilations and translations of the auto-correlation functions of the compactly supported wavelets. Although these auto-correlation functions do not constitute an orthonormal basis of $\mathbf{L}^2(\mathbf{R})$, there exists a simple decomposition and reconstruction algorithm as well as an algorithm for converting this expansion into the orthonormal shell expansion on each scale separately. A new interpretation of Dubuc's iterative interpolation scheme is discussed in Section IV. In Section V we formulate our approach to the

reconstruction of signals from zero-crossings (and slopes at these points) in their auto-correlation shell representations and give several examples.

II An Orthonormal Shell: A Shift-Invariant Representation Using Orthonormal Wavelets

In many image processing applications (e.g. pattern matching), a useful signal representation must be shift invariant. Although coefficients of orthonormal wavelet expansions are not shift invariant, the wavelet coefficients of all N circulant shifts of a vector of size $N = 2^n$ may be computed in $O(N \log_2 N)$ operations [23]. Once all wavelet coefficients of N circulant shifts of the vector are computed, we may use them for a variety of applications where the shift invariance is essential. By introducing the notion of a *shell*, a redundant but shift-invariant family of functions, the algorithm of [23] may be viewed as an expansion of a vector in such a shell. The notion of "frame" is not adequate for our purposes since the shell is overly redundant.

We note that the computational diagram of this algorithm is essentially identical to the Hierarchical Discrete Correlation scheme (HDC) [24] of P. Burt, which was designed for efficient correlation of images at multiple scales. We also note that the HDC scheme was proposed prior to the Laplacian pyramid scheme [25] which, in turn, stimulated the development of the multiresolution analysis [26] and of the orthonormal bases of the compactly supported wavelets [5].

First, let us briefly review the properties of the compactly supported wavelets (for details we refer to [5]). The orthonormal basis of compactly supported wavelets of $\mathbf{L}^2(\mathbf{R})$ is formed by the dilation and translation of a single function $\psi(x)$,

$$\psi_{j,k}(x) = 2^{-j/2}\psi(2^{-j}x - k), \tag{2.1}$$

where $j, k \in \mathbf{Z}$. The function $\psi(x)$ has a companion, the scaling function $\varphi(x)$.

The wavelet basis induces a multiresolution analysis on $\mathbf{L}^2(\mathbf{R})$ [27], [26], i.e., the decomposition of the Hilbert space $\mathbf{L}^2(\mathbf{R})$ into a chain of closed subspaces

$$\cdots \subset \mathbf{V}_2 \subset \mathbf{V}_1 \subset \mathbf{V}_0 \subset \mathbf{V}_{-1} \subset \mathbf{V}_{-2} \subset \cdots \tag{2.2}$$

such that

$$\bigcap_{j\in\mathbf{Z}} \mathbf{V}_j = \{0\}, \quad \overline{\bigcup_{j\in\mathbf{Z}}} \mathbf{V}_j = \mathbf{L}^2(\mathbf{R}). \tag{2.3}$$

By defining $\mathbf{W}_j$ as an orthogonal complement of $\mathbf{V}_j$ in $\mathbf{V}_{j-1}$,

$$\mathbf{V}_{j-1} = \mathbf{V}_j \bigoplus \mathbf{W}_j, \tag{2.4}$$

the space $\mathbf{L}^2(\mathbf{R})$ is represented as a direct sum

$$\mathbf{L}^2(\mathbf{R}) = \bigoplus_{j\in\mathbf{Z}} \mathbf{W}_j. \tag{2.5}$$

On each fixed scale j, the wavelets $\{\psi_{j,k}(x)\}_{k\in\mathbf{Z}}$ form an orthonormal basis of $\mathbf{W}_j$ and the functions $\{\varphi_{j,k}(x) = 2^{-j/2}\varphi(2^{-j}x - k)\}_{k\in\mathbf{Z}}$ form an orthonormal basis of $\mathbf{V}_j$. In addition, the function ψ has M vanishing moments

$$\int_{-\infty}^{+\infty} \psi(x)x^m dx = 0, \qquad m = 0, \ldots, M-1. \tag{2.6}$$

Due to the fact that $\mathbf{V}_j, \mathbf{W}_j \subset \mathbf{V}_{j-1}$, the functions φ and ψ satisfy the following relations:

$$\varphi(x) = \sqrt{2} \sum_{k=0}^{L-1} h_k \varphi(2x-k), \tag{2.7}$$

$$\psi(x) = \sqrt{2} \sum_{k=0}^{L-1} g_k \varphi(2x-k), \tag{2.8}$$

where

$$g_k = (-1)^k h_{L-k-1}, \qquad k = 0, \ldots, L-1. \tag{2.9}$$

The number of coefficients L in (2.7) and (2.8) is related to the number of vanishing moments M and for the wavelets in [5] $L = 2M$. If additional conditions are imposed (see [28] for an example), then the relation might be different, but L is always even.

The coefficients $H = \{h_k\}_{0 \le k \le L-1}$ and $G = \{g_k\}_{0 \le k \le L-1}$ in (2.7) and (2.8) are quadrature mirror filters since they satisfy the equation

$$|m_0(\xi)|^2 + |m_1(\xi)|^2 = 1, \tag{2.10}$$

where the 2π-periodic functions m_0 and m_1 are defined as

$$m_0(\xi) = \frac{1}{\sqrt{2}} \sum_{k=0}^{L-1} h_k \mathrm{e}^{\mathrm{i}k\xi}, \tag{2.11}$$

and

$$m_1(\xi) = \frac{1}{\sqrt{2}} \sum_{k=0}^{L-1} g_k \mathrm{e}^{\mathrm{i}k\xi} = \mathrm{e}^{\mathrm{i}(\xi+\pi)} \overline{m_0(\xi+\pi)}. \tag{2.12}$$

A. The orthonormal shell

In practical applications there is always the finest scale of interest and, therefore, it is sufficient to consider only shifts by multiples of some fixed unit. Throughout this paper we will assume that the number of scales is finite and that there exist a finest and a coarsest scale of interest. Without loss of generality, we will assume that the finest scale is described by the $N(= 2^n)$ dimensional subspace $\mathbf{V}_0 \subset \mathbf{L}^2(\mathbf{R})$ and consider only circulant shifts on $\mathbf{V}_0$. In this case, the multiresolution decomposition of the space $\mathbf{V}_0$ may be written as

$$\mathbf{V}_0 = \mathbf{V}_{n_0} \bigoplus_{j=1}^{n_0} \mathbf{W}_j, \tag{2.13}$$

where $1 \le n_0 \le n$ and the subspace $\mathbf{V}_{n_0}$ describes the coarsest scale.

Since the functions

$$\{\psi_{j,k}(x)\}_{1 \le j \le n_0,\ 0 \le k \le 2^{n-j}-1} \quad \text{and} \quad \{\varphi_{n_0,k}(x)\}_{0 \le k \le 2^{n-n_0}-1}, \tag{2.14}$$

form an orthonormal basis of $\mathbf{V}_0$, for any vector $f \in \mathbf{V}_0$ represented by

$$f(x) = \sum_{k=0}^{N-1} s_k^0 \varphi_{0,k}(x), \tag{2.15}$$

we have the following relation:

$$\|f\|^2 = \sum_{j=1}^{n_0} \sum_{k=0}^{2^{n-j}-1} (d_k^j)^2 + \sum_{k=0}^{2^{n-n_0}-1} (s_k^{n_0})^2. \tag{2.16}$$

The coefficients s_k^j and d_k^j in (2.16) are defined as

$$s_k^j = \int f(x) \varphi_{j,k}(x) dx, \tag{2.17}$$

and

$$d_k^j = \int f(x) \psi_{j,k}(x) dx, \tag{2.18}$$

for $j = 1, 2, \ldots, n_0$ and $k = 0, 1, \ldots, 2^{n-j} - 1$, and the norm is defined as

$$\|f\| = \left(\sum_{k=0}^{N-1} (s_k^0)^2 \right)^{1/2}. \tag{2.19}$$

We refer to the set of coefficients $\{d_k^j\}_{1 \le j \le n_0,\ 0 \le k \le 2^{n-j}-1}$ and $\{s_k^{n_0}\}_{0 \le k \le 2^{n-n_0}-1}$ as orthonormal wavelet coefficients.

We now consider a family of functions

$$\left\{\widetilde{\psi}_{j,k}(x)\right\}_{1 \le j \le n_0,\ 0 \le k \le N-1} \quad \text{and} \quad \{\widetilde{\varphi}_{n_0,k}(x)\}_{0 \le k \le N-1}, \tag{2.20}$$

where

$$\widetilde{\psi}_{j,k}(x) = 2^{-j/2} \psi(2^{-j}(x-k)), \tag{2.21}$$

and

$$\widetilde{\varphi}_{n_0,k}(x) = 2^{-n_0/2} \varphi(2^{-n_0}(x-k)). \tag{2.22}$$

We call this family a *shell* of the orthonormal wavelets for shifts in $\mathbf{V}_0$. Henceforth, we call this family an *orthonormal shell* for short.

Let us define the following norm,

$$\|f\|_{\mathcal{S}}^2 = \sum_{j=1}^{n_0} 2^{-j} \sum_{k=0}^{N-1} (d_k^j)^2 + 2^{-n_0} \sum_{k=0}^{N-1} (s_k^{n_0})^2, \tag{2.23}$$

where the coefficients s_k^j and d_k^j are defined as

$$s_k^j = \int f(x) \widetilde{\varphi}_{j,k}(x) dx, \tag{2.24}$$

and

$$d_k^j = \int f(x)\tilde{\psi}_{j,k}(x)dx, \tag{2.25}$$

We refer to the set of coefficients $\{d_k^j\}_{1\le j\le n_0,\ 0\le k\le N-1}$ and $\{s_k^{n_0}\}_{0\le k\le N-1}$ as the *orthonormal shell coeffcients*. The factor 2^{-j} in (2.23) is used to offset the redundancy of this representation. In other words, at the j-th scale this representation is 2^j times more redundant than the orthonormal wavelet representation. It is clear that

$$\|f\|^2 = \|f\|_{\mathcal{S}}^2. \tag{2.26}$$

B. A fast algorithm for expanding into the orthonormal shell

Let us assume that the orthonormal wavelet coefficients of the finest scale $\{s_k^0\}_{0\le k\le N-1}$ are given as an original signal and let us consider the function $f = \sum_{k=0}^{N-1} s_k^0 \varphi_{0,k} \in \mathbf{V}_0$. To obtain the orthonormal shell coefficients of this function f, we use the quadrature mirror filters $H = \{h_l\}_{0\le l\le L-1}$ and $G = \{g_l\}_{0\le l\le L-1}$ (associated with the orthonormal basis of compactly supported wavelets) and compute

$$s_k^j = \sum_{l=0}^{L-1} h_l s_{k+2^{j-1}l}^{j-1}, \tag{2.27}$$

and

$$d_k^j = \sum_{l=0}^{L-1} g_l s_{k+2^{j-1}l}^{j-1}, \tag{2.28}$$

for $j = 1, \ldots, n_0,\ k = 0, \ldots, N-1$. Clearly, computations via (2.27) and (2.28) require $2Nn_0 \le 2N\log_2 N$ operations. The diagram for computing these coefficients via (2.27) and (2.28) is illustrated in Figure 1.

Using (2.11) and (2.12), we rewrite (2.27) and (2.28) in the Fourier domain,

$$\hat{s}^j(\xi) = \sqrt{2}\ \overline{m_0(2^{j-1}\xi)}\ \hat{s}^{j-1}(\xi), \tag{2.29}$$

$$\hat{d}^j(\xi) = \sqrt{2}\ \overline{m_1(2^{j-1}\xi)}\ \hat{s}^{j-1}(\xi). \tag{2.30}$$

Let us show that we have computed the orthonormal wavelet coefficients of all circulant shifts of the function f. Since the algorithmic structures for computing the coefficients $\{s_k^j\}$ and $\{d_k^j\}$ are exactly the same, we consider only $\{d_k^j\}$. At the first scale, we have

$$d_k^1 = \sum_{l=0}^{L-1} g_l s_{k+l}^0. \tag{2.31}$$

We rewrite (2.31) as

$$d_{2k}^1 = \sum_{l=0}^{L-1} g_l s_{2k+l}^0, \tag{2.32}$$

and

$$d_{2k+1}^1 = \sum_{l=0}^{L-1} g_l s_{2k+1+l}^0, \tag{2.33}$$

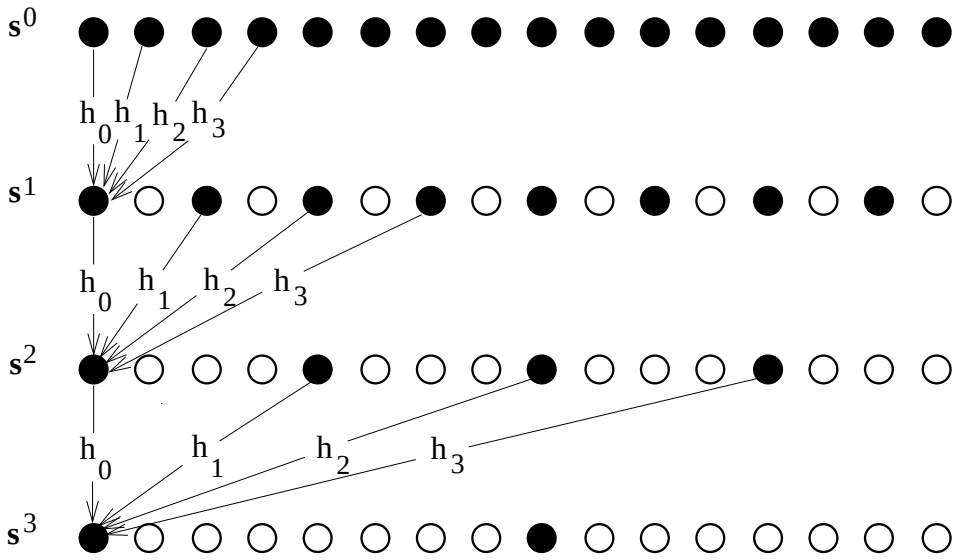

Figure 1: A scheme illustrating the algorithm for expanding into the orthonormal shell. Using the quadrature mirror filter $H = \{h_0, h_1, h_2, h_3\}$, all points are computed for the orthonormal shell, whereas only points marked by $\bullet$ are computed for the orthonormal wavelet expansion.

for $k = 0, \ldots, N/2 - 1$. The right hand side of (2.32) coincides with the computation of the orthonormal wavelet coefficients of $f(x)$, whereas (2.33) produces the orthonormal wavelet coefficients of the *shifted* signal $f(x+1)$. It is clear that the sequence $\{d^1_{2k}\}$ contains all the orthonormal wavelet coefficients that appear if $f(x)$ is circularly shifted by $2, 4, \ldots$, and the sequence $\{d^1_{2k+1}\}$ contains all the orthonormal wavelet coefficients for odd shifts $(1, 3, \ldots)$.

Similarly, at the j-th scale, we may rewrite d^j_k as

$$d^j_{2^j k} = \sum_{l=0}^{L-1} g_l s^{j-1}_{2^{j-1}(2k+l)}, \tag{2.34}$$

$$d^j_{2^j k+1} = \sum_{l=0}^{L-1} g_l s^{j-1}_{2^{j-1}(2k+l)+1}, \tag{2.35}$$

$$\vdots$$

$$d^j_{2^j k+2^j-1} = \sum_{l=0}^{L-1} g_l s^{j-1}_{2^{j-1}(2k+l)+2^j-1}, \tag{2.36}$$

for $k = 0, \ldots, 2^{n-j}$. Now the sequences $\{d^j_{2^j k}\}$, $\{d^j_{2^j k+1}\}$, $\ldots$, $\{d^j_{2^j k+2^j-1}\}$ contain the orthonormal wavelet coefficients of the j-th scale of the signal shifted by $0, 1, \ldots, 2^j - 1$, respectively. Therefore, the set $\{d^j_k\}_{1 \le j \le n_0,\ 0 \le k \le N-1}$ and $\{s^{n_0}_k\}_{0 \le k \le N-1}$ contains all the coefficients of the orthonormal wavelet expansion of $f(x), f(x+1), \ldots, f(x+N-1)$.

Figure 2 illustrates the shift invariance of the representation. In Figure 2 we use the quadrature mirror filters with two vanishing moments and of length $L = 4$ and depth of expansions

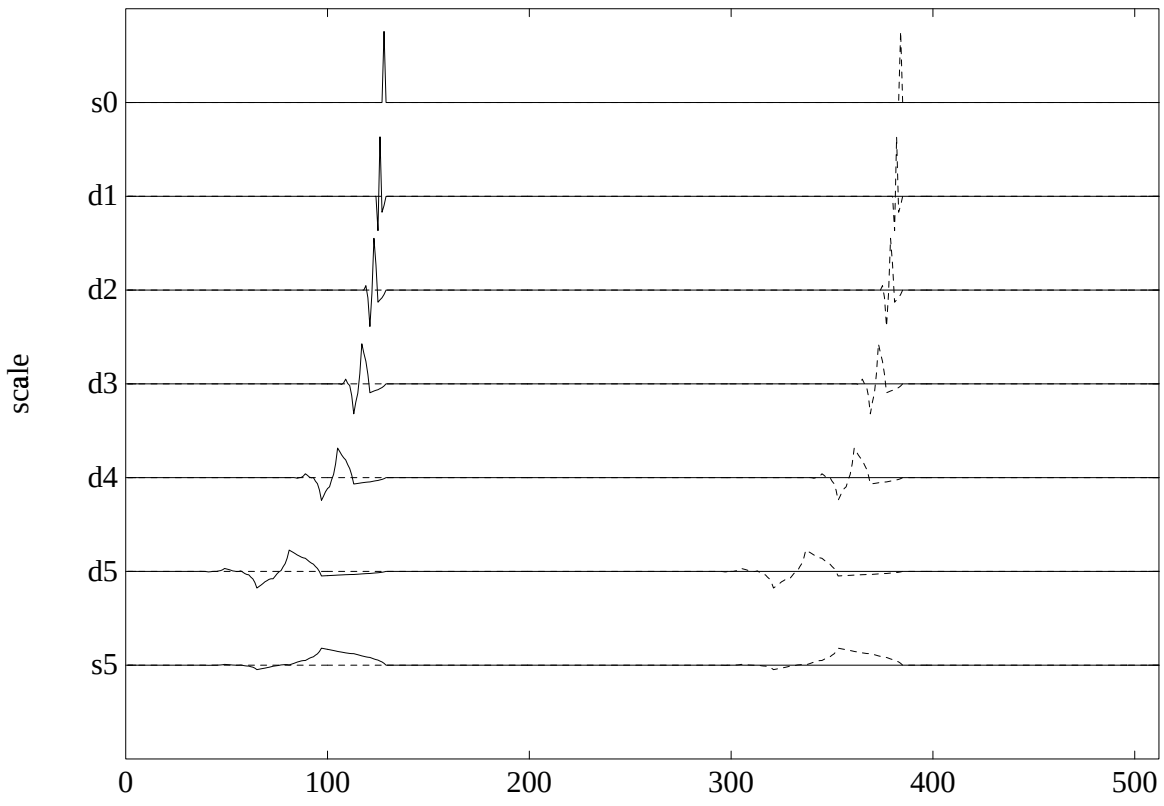

Figure 2: The expansion of two unit impulses into the orthonormal shell using the Daubechies's wavelet with two vanishing moments and $L = 4$.

$n_0 = 5$. The top row shows the original impulses. Dotted lines highlight the expansion of the shifted impulse. Clearly, the shift in the original signal is preserved at each scale. Note that in Figure 2 we see the mirror images of wavelets with details appropriate at corresponding scales. It is clear that due to "rough" shapes of wavelets there might be "too many" zero-crossings. Also, the positions of peaks are shifted across the scales due to the asymmetry of the wavelets.

The following proposition shows the relationship between the original signal $\{s_k^0\}$ and the coefficients of the orthonormal shell expansion of this signal.

Proposition 1 *For any function $f \in \mathbf{V}_0$, $f(x) = \sum_{k=0}^{N-1} s_k^0 \varphi(x-k)$, the coefficients $\{s_k^j\}$ and $\{d_k^j\}$ defined in (2.24) and (2.25) satisfy the following identities*

$$\sum_{k=0}^{N-1} s_k^j \widetilde{\varphi}_{0,k}^{\triangleleft} = \sum_{k=0}^{N-1} s_k^0 \widetilde{\varphi}_{j,k}^{\triangleleft}, \tag{2.37}$$

and

$$\sum_{k=0}^{N-1} d_k^j \widetilde{\varphi}_{0,k}^{\triangleleft} = \sum_{k=0}^{N-1} s_k^0 \widetilde{\psi}_{j,k}^{\triangleleft}, \tag{2.38}$$

where $\widetilde{\varphi}_{0,k}(x) = \varphi_{0,k}(x)$, $\widetilde{\varphi}^{\triangleleft}(x) = \widetilde{\varphi}(-x)$, and $\widetilde{\varphi}_{j,k}$, $\widetilde{\psi}_{j,k}$ are defined in (2.22) and (2.21).

Proof. Recursively applying (2.29) and (2.30), the relationship between $\hat{s}^0(\xi)$ and $\hat{s}^j(\xi)$, $\hat{d}^j(\xi)$ may be written as

$$\hat{s}^j(\xi) = \hat{s}^0(\xi)\ 2^{j/2} \prod_{l=1}^{j} \overline{m_0(2^{l-1}\xi)}, \tag{2.39}$$

$$\hat{d}^j(\xi) = \hat{s}^0(\xi)\ 2^{j/2}\ \overline{m_1(2^{j-1}\xi)} \prod_{l=1}^{j-1} \overline{m_0(2^{l-1}\xi)}, \tag{2.40}$$

for $k = 0, \ldots, N-1$. By multiplying (2.39) by $\overline{\hat{\varphi}(\xi)}$, we have

$$\hat{s}^j(\xi)\overline{\hat{\varphi}(\xi)} = \hat{s}^0(\xi)\ 2^{j/2} \prod_{l=1}^{j} \overline{m_0(2^{l-1}\xi)}\ \overline{\hat{\varphi}(\xi)} = \hat{s}^0(\xi)\ 2^{j/2}\overline{\hat{\varphi}(2^j\xi)}, \tag{2.41}$$

where we have used the identity

$$\hat{\varphi}(\xi) = \prod_{l=1}^{\infty} m_0(2^{-l}\xi). \tag{2.42}$$

The inverse Fourier transform of (2.41) yields (2.37). The relation (2.38) may be derived similarly.

Figure 2 illustrates the proposition. By applying the proposition to the sequence $\{s_k^0 = \delta_{k_0,k}\}$, we have an expansion $\{2^{-j/2}\varphi(2^{-j}(k_0 - x))\}_{1 \le j \le n_0}$ and $2^{-n_0/2}\varphi(2^{-n_0}(k_0 - x))$. Therefore, we see the mirror images of the basis functions themselves.

C. A fast reconstruction algorithm

Given the coefficients $\{d_k^j\}_{1\le j\le n_0,\ 0\le k\le N-1}$ and $\{s_k^{n_0}\}_{0\le k\le N-1}$, we adopt the most natural reconstruction algorithm to recover the original vector $\{s_k^0\}_{0\le k\le N-1}$. Let us use the expressions in the Fourier domain (2.29) and (2.30). Multiplying (2.29) by the filter $m_0(2^{j-1}\xi)$, (2.30) by the filter $m_1(2^{j-1}\xi)$, adding the results, and using (2.10), we obtain

$$m_0(2^{j-1}\xi)\ \hat{s}^j(\xi) + m_1(2^{j-1}\xi)\ \hat{d}^j(\xi) = \sqrt{2}\ \hat{s}^{j-1}(\xi). \tag{2.43}$$

This expression is equivalent to

$$s_k^{j-1} = \frac{1}{2}\sum_{l=0}^{L-1}(h_l s_{k-2^{j-1}l}^j + g_l d_{k-2^{j-1}l}^j), \tag{2.44}$$

for $j = 1,\dots,n_0,\ k = 0,\dots,N-1$. As shown in the previous subsection, the orthonormal shell coefficients on the j-th scale are twice as redundant as on the $(j-1)$-th scale, and the factor $\frac{1}{2}$ in (2.44) accounts for this.

III An Auto-Correlation Shell of Compactly Supported Wavelets

The representation of a signal in the orthonormal shell is shift invariant. This representation, however, has several drawbacks for certain applications, such as detecting and characterizing edges (or singularities) in the signal, where the scale-to-scale analysis of the coefficients is necessary [29],[20],[21]. This representation lacks symmetry because of the asymmetric shapes of compactly supported wavelets. It results in a rather complicated representation even in the case of the unit impulse sequence, as may be seen in Figure 2. Also, because of the "rough" shape of compactly supported wavelets, there might be "too many" zero-crossings in this representation.

In this section we introduce the notion of an *auto-correlation shell* of compactly supported wavelets, that is, a shell formed by dilations and translations of the auto-correlation functions of compactly supported wavelets. The decomposition filters associated with the auto-correlation function of compactly supported wavelets naturally have symmetric shapes which simplifies the scale-to-scale analysis of the coefficients. One of the interesting features of this representation is its convertibility to the orthonormal shell of the corresponding compactly supported wavelets on each scale independently of other scales. The algorithm for such conversion is discussed in detail in this section. After describing the fast decomposition and reconstruction algorithms of signals in the auto-correlation shell of compactly supported wavelets, we investigate the subsampled representation. It turns out that it is possible to reconstruct the original signal, if we store a single additional number at each scale, the Nyquist frequency component of the signal on that scale.

A. Properties of the auto-correlation functions of compactly supported wavelets

First let us summarize the properties of the auto-correlation functions of a compactly supported scaling function $\varphi(x)$ and the corresponding wavelet $\psi(x)$. By definition of the auto-correlation function, we have

$$\Phi(x) = \int_{-\infty}^{+\infty} \varphi(y)\varphi(y-x)dy, \tag{3.1}$$

$$\Psi(x) = \int_{-\infty}^{+\infty} \psi(y)\psi(y-x)dy. \tag{3.2}$$

Given the fact that $\{\varphi(x-k)\}_{0\le k\le N-1}$ and $\{\psi(x-k)\}_{0\le k\le N-1}$ form orthonormal bases on $\mathbf{V}_0$ and $\mathbf{W}_0$ respectively, we immediately obtain that at integer points

$$\Phi(k) = \delta_{0k}, \tag{3.3}$$

and

$$\Psi(k) = \delta_{0k}, \tag{3.4}$$

where δ_{0k} denotes the Kronecker delta.

The Fourier transforms of the auto-correlation functions in (3.1) and (3.2) are as follows:

$$\hat{\Phi}(\xi) = |\hat{\varphi}(\xi)|^2, \tag{3.5}$$

and

$$\hat{\Psi}(\xi) = |\hat{\psi}(\xi)|^2. \tag{3.6}$$

By taking the Fourier transforms of (2.7) and (2.8), we have

$$\hat{\varphi}(\xi) = m_0(\xi/2)\hat{\varphi}(\xi/2), \tag{3.7}$$

$$\hat{\psi}(\xi) = m_1(\xi/2)\hat{\varphi}(\xi/2). \tag{3.8}$$

Using (3.7), (3.8), we obtain

$$\hat{\Phi}(\xi) = |m_0(\xi/2)|^2\hat{\Phi}(\xi/2), \tag{3.9}$$

$$\hat{\Psi}(\xi) = |m_1(\xi/2)|^2\hat{\Phi}(\xi/2). \tag{3.10}$$

Equation (2.10) also implies that

$$\hat{\Phi}(\xi) + \hat{\Psi}(\xi) = \hat{\Phi}(\xi/2). \tag{3.11}$$

Since $|m_0(\xi)|^2$ is an even function, we have

$$|m_0(\xi)|^2 = \frac{1}{2} + \frac{1}{2}\sum_{k=1}^{L/2} a_{2k-1}\cos(2k-1)\xi, \tag{3.12}$$

where $\{a_k\}$ are the auto-correlation coefficients of the filter H,

$$a_k = 2\sum_{l=0}^{L-1-k} h_l h_{l+k} \qquad \text{for} \quad k = 1, \ldots, L-1, \tag{3.13}$$

and

$$a_{2k} = 0 \qquad \text{for} \quad k = 1, \ldots, L/2-1. \tag{3.14}$$

The coefficients $\{a_{2k-1}\}_{1\le k\le L/2}$ were used in [23] for computing representations of derivatives and convolution operators in the bases of compactly supported wavelets.

Using (2.7), (3.9), and (3.12), it is easy to derive

$$\Phi(x) = \Phi(2x) + \frac{1}{2}\sum_{l=1}^{L/2} a_{2l-1}\left(\Phi(2x-2l+1) + \Phi(2x+2l-1)\right), \tag{3.15}$$

and

$$\Psi(x) = \Phi(2x) - \frac{1}{2}\sum_{l=1}^{L/2} a_{2l-1}\left(\Phi(2x-2l+1) + \Phi(2x+2l-1)\right). \tag{3.16}$$

By direct examination of (3.15) and (3.16), we obtain that both Φ and Ψ are supported within the interval $[-L+1, L-1]$.

Finally, $\Phi(x)$ and $\Psi(x)$ have vanishing moments [23], namely

$$\mathcal{M}_\Psi^m = \int_{-\infty}^{+\infty} x^m \Psi(x) dx = 0, \qquad \text{for} \quad 0 \le m \le L-1, \tag{3.17}$$

$$\mathcal{M}_\Phi^m = \int_{-\infty}^{+\infty} x^m \Phi(x) dx = 0, \qquad \text{for} \quad 1 \le m \le L-1, \tag{3.18}$$

and

$$\int_{-\infty}^{+\infty} \Phi(x) dx = 1. \tag{3.19}$$

Since L consecutive moments of the auto-correlation function $\Psi(x)$ vanish (3.17), we have

$$\hat{\Psi}(\xi) = O(\xi^L). \tag{3.20}$$

Therefore, $\hat{\Psi}(\xi)$ may be viewed as the symbol of a pseudo-differential operator which behaves like an approximation of the derivative operator $(d/dx)^L$. We note that due to its definition this operator may be calculated recursively. The convolution with the function $\Psi(x)$ has two properties useful in edge detection (see [13]): it behaves essentially like a differential operator in detecting spatial intensity changes and it is designed to act at any desired scale.

Finally, we display functions $\Phi(x)$, $\varphi(x)$, $\Psi(x)$, $\psi(x)$, and the magnitudes of their Fourier transforms in Figures 3 and 4. In these figures, we have used the Daubechies's wavelet with two vanishing moments and $L = 4$. It is easy to see that the auto-correlation functions $\Phi(x)$ and $\Psi(x)$ are smoother than the functions $\varphi(x)$ and $\psi(x)$ and $\hat{\Phi}(\xi)$ and $\hat{\Psi}(\xi)$ decay faster than $\hat{\varphi}(\xi)$ and $\hat{\psi}(\xi)$ respectively. We also note that both $\Phi(x)$ and $\Psi(x)$ are even.

Remark 1 It follows from (3.11) or (3.15) and (3.16) that

$$\Psi(x) = 2\Phi(2x) - \Phi(x). \tag{3.21}$$

This may be compared with the approximation of the Laplacian of a Gaussian function (the so-called Mexican-hat function) by the Difference of two Gaussian functions (the so-called DOG function) as

$$\frac{d^2}{dx^2} G(x;\sigma) \approx G(x;a\sigma) - G(x;\sigma) \tag{3.22}$$

$$= aG(ax;\sigma) - G(x;\sigma), \tag{3.23}$$

where

$$G(x;\sigma) = \frac{1}{\sqrt{2\pi}\sigma} \mathrm{e}^{-x^2/2\sigma^2}, \tag{3.24}$$

and $a = 1.6$ as Marr suggested in [13].

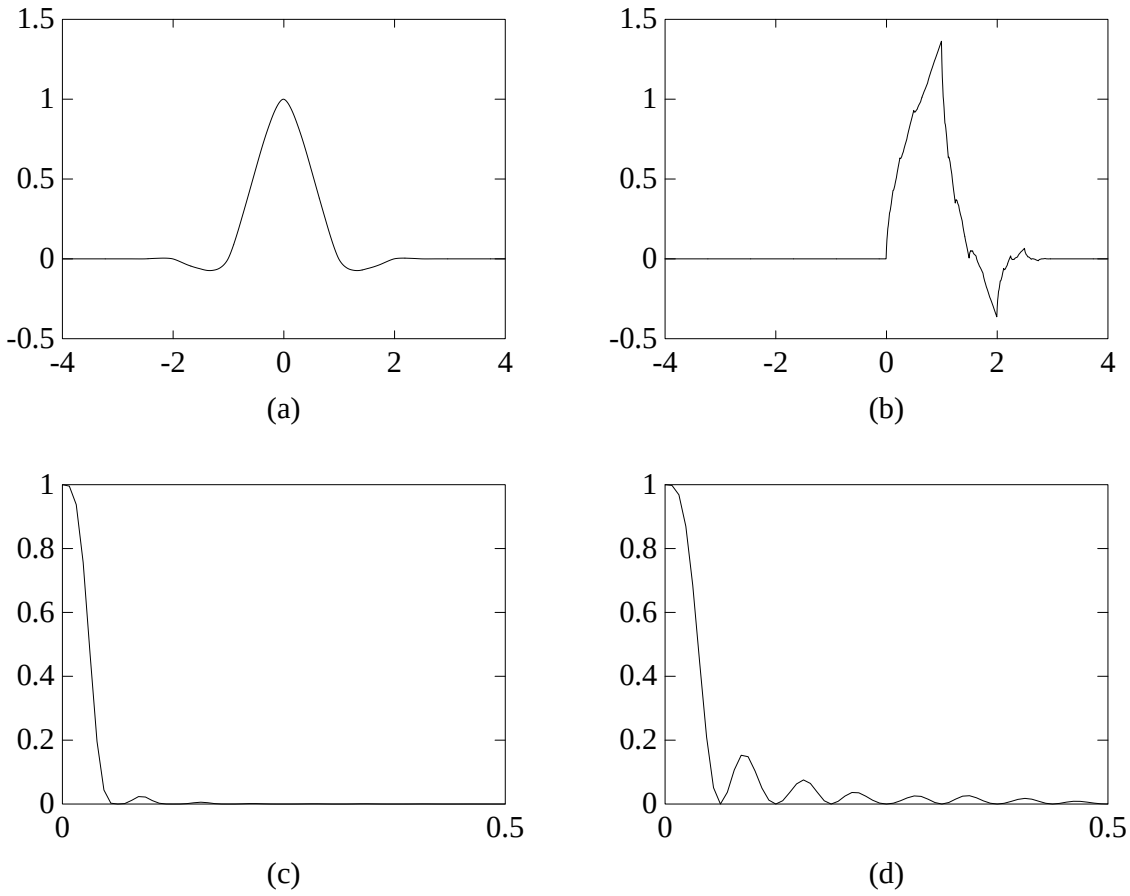

Figure 3: Plots of the auto-correlation function $\Phi(x)$ and the Daubechies's scaling function $\varphi(x)$ with $L = 4$. (a) $\Phi(x)$. (b) $\varphi(x)$. (c) Magnitude of the Fourier transform of $\Phi(x)$. (d) Magnitude of the Fourier transform of $\varphi(x)$.

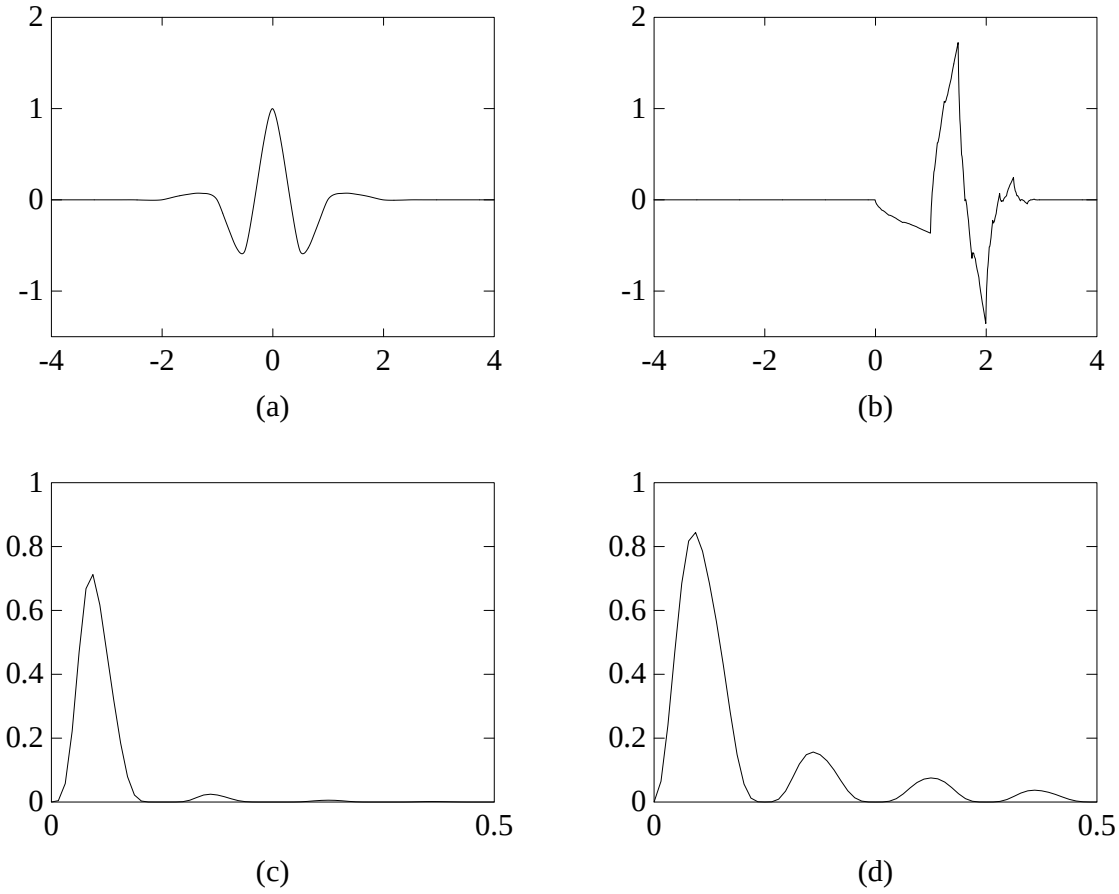

Figure 4: Plots of the auto-correlation function $\Psi(x)$ and the Daubechies's wavelet $\psi(x)$ with two vanishing moments and $L = 4$. (a) $\Psi(x)$. (b) $\psi(x)$. (c) Magnitude of the Fourier transform of $\Psi(x)$. (d) Magnitude of the Fourier transform of $\psi(x)$.

B. The auto-correlation shell of compactly supported wavelets

By analogy with the previous section, let us now consider the following family of functions,

$$\left\{\widetilde{\Psi}_{j,k}(x)\right\}_{1\le j\le n_0,\ 0\le k\le N-1} \quad \text{and} \quad \left\{\widetilde{\Phi}_{n_0,k}(x)\right\}_{0\le k\le N-1}, \tag{3.25}$$

where

$$\widetilde{\Psi}_{j,k}(x) = 2^{-j/2}\Psi(2^{-j}(x-k)), \tag{3.26}$$

and

$$\widetilde{\Phi}_{n_0,k}(x) = 2^{-n_0/2}\Phi(2^{-n_0}(x-k)). \tag{3.27}$$

We call this family a shell of auto-correlations of compactly supported wavelets for shifts in $\mathbf{V}_0$. Henceforth, we call this family an *auto-correlation shell* for short.

The relation to the orthonormal shell

Let us now consider the relation between the auto-correlation shell and the orthonormal shell. Let $f \in \mathbf{V}_0$ so that

$$f(x) = \sum_{k=0}^{N-1} s_k^0 \varphi(x-k), \tag{3.28}$$

and consider the function $\mathcal{A}f$,

$$\mathcal{A}f(x) = \sum_{k=0}^{N-1} s_k^0 \Phi(x-k). \tag{3.29}$$

These two functions are related via

$$\mathcal{A}f(x) = \int f(y)\varphi(y-x)dy, \tag{3.30}$$

and

$$\mathcal{A}f(k) = s_k^0, \qquad \text{for} \quad k = 0, 1, \ldots, N-1. \tag{3.31}$$

Similarly at the scale j, let us define functions $f_s^j(x)$ and $f_d^j(x)$ using the orthonormal shell coefficients s_k^j and d_k^j,

$$f_s^j(x) = \sum_{k=0}^{N-1} s_k^j \varphi(x-k), \tag{3.32}$$

and

$$f_d^j(x) = \sum_{k=0}^{N-1} d_k^j \varphi(x-k). \tag{3.33}$$

By correlating the functions $f_s^j(x)$ and $f_d^j(x)$ with the functions $2^{-j}\varphi(2^{-j}x)$ and $2^{-j}\psi(2^{-j}x)$ on each scale j, we obtain

$$\mathcal{A}_s^j f(x) = \int f_s^j(y)\ 2^{-j}\varphi(2^{-j}(y-x))dy = \sum_{k=0}^{N-1} S_k^j \Phi(x-k), \tag{3.34}$$

and

$$\mathcal{A}_d^j f(x) = \int f_d^j(y)\ 2^{-j}\psi(2^{-j}(y-x))dy = \sum_{k=0}^{N-1} D_k^j \Phi(x-k), \tag{3.35}$$

where we define the coefficients $\{S_k^j\}$ and $\{D_k^j\}$ to be the *auto-correlation shell coefficients* (averages and differences). From (3.3), the coefficients $\{S_k^j\}$ and $\{D_k^j\}$ are the values of $\mathcal{A}_s^j f(x)$ and $\mathcal{A}_d^j f(x)$ at integer points

$$S_k^j = \mathcal{A}_s^j f(k) = \int f_s^j(y)\ 2^{-j}\varphi(2^{-j}(y-k))dy, \tag{3.36}$$

and

$$D_k^j = \mathcal{A}_d^j f(k) = \int f_d^j(y)\ 2^{-j}\psi(2^{-j}(y-k))dy. \tag{3.37}$$

To summarize, the coefficients $\{S_k^j\}$ and $\{D_k^j\}$ may be obtained as follows:

step 1. Expand the function $f \in \mathbf{V}_0$ in the orthonormal shell and obtain the coefficients $\{s_k^j\}$ and $\{d_k^j\}$ (see Section II).

step 2. Expand the unit impulse $\{\delta_{0k}\}$ in the orthonormal shell and obtain the coefficients $\{v_k^j\}$ and $\{w_k^j\}$, which are the values of $2^{-j/2}\varphi^{\triangleleft}(2^{-j}x)$ and $2^{-j/2}\psi^{\triangleleft}(2^{-j}x)$ at integer points x.

step 3. For each scale j, correlate the coefficients $\{s_k^j\}$ and $\{d_k^j\}$ with the coefficients of the unit impulse $\{v_k^j\}$ and $\{w_k^j\}$ respectively, and multiply the results by the factor $2^{-j/2}$.

Remark 2 In applications of auto-correlation shell representations, one may assume that the original continuous signal is the function $\mathcal{A}f(x)$ rather than $f(x)$. In this case $\{s_k^0\}$ are the values of $\mathcal{A}f(x)$ at integer points.

A fast algorithm for expanding in an auto-correlation shell

Let us now derive a fast algorithm for expanding in an auto-correlation shell, i.e., the pyramid algorithm for computing $\{S_k^j\}$ and $\{D_k^j\}$ from $\{S_k^{j-1}\}$. First, let us define the coefficients $\{p_k\}$ and $\{q_k\}$ by rewriting the equations (3.15) and (3.16) as

$$\frac{1}{\sqrt{2}}\Phi(x/2) = \sum_{k=-L+1}^{L-1} p_k \Phi(x-k), \tag{3.38}$$

$$\frac{1}{\sqrt{2}}\Psi(x/2) = \sum_{k=-L+1}^{L-1} q_k \Phi(x-k), \tag{3.39}$$

where

$$p_k = \begin{cases} 2^{-1/2} & \text{for } k = 0 \\ 2^{-3/2} a_{|k|} & \text{for } k = \pm 1, \pm 3, \ldots, \pm(L-1) \\ 0 & \text{for } k = \pm 2, \pm 4, \ldots, \pm(L-2) \end{cases} \tag{3.40}$$

$$q_k = \begin{cases} 2^{-1/2} & \text{for } k = 0 \\ -p_k & \text{otherwise} \end{cases} \tag{3.41}$$

We view these coefficients as filters $P = \{p_k\}_{-L+1 \le k \le L-1}$ and $Q = \{q_k\}_{-L+1 \le k \le L-1}$. It is clear that $p_k = p_{-k}$ and $q_k = q_{-k}$ (see (3.40) and (3.41)) and so there are only $L/2+1$ distinct non-zero coefficients. By taking Fourier transforms of both sides of (3.38) and (3.39) and using (3.9) and (3.10), we obtain

$$\sqrt{2}|m_0(\xi)|^2 = \sum_{k=-L+1}^{L-1} p_k \mathrm{e}^{\mathrm{i}k\xi}, \tag{3.42}$$

and

$$\sqrt{2}|m_1(\xi)|^2 = \sum_{k=-L+1}^{L-1} q_k \mathrm{e}^{\mathrm{i}k\xi}. \tag{3.43}$$

Thus, using Φ and Ψ for the decomposition is equivalent to viewing $\sqrt{2}|m_0(\xi)|^2$ and $\sqrt{2}|m_1(\xi)|^2$ as decomposition filters instead of $m_0(\xi)$ and $m_1(\xi)$ in the orthonormal case. We note that the pair of filters $\sqrt{2}|m_0(\xi)|^2$ and $\sqrt{2}|m_1(\xi)|^2$ is not a quadrature mirror pair since $2|m_0(\xi)|^4 + 2|m_1(\xi)|^4 \neq 1$. Using the filters P and Q, we obtain the pyramid algorithm for expanding into the auto-correlation shell,

$$S_k^j = \sum_{l=-L+1}^{L-1} p_l S_{k+2^{j-1}l}^{j-1}, \tag{3.44}$$

and

$$D_k^j = \sum_{l=-L+1}^{L-1} q_l S_{k+2^{j-1}l}^{j-1}. \tag{3.45}$$

As an example of the coefficients $\{p_k\}$, for Daubechies's wavelets with two vanishing moments, $L = 4$ and the coefficients are $2^{-1/2}(-\frac{1}{16}, 0, \frac{9}{16}, 1, \frac{9}{16}, 0, -\frac{1}{16})$.

The direct conversion from an auto-correlation shell to an orthonormal shell

We now consider an algorithm for the direct conversion of $\{S_k^j\}$ and $\{D_k^j\}$ to $\{s_k^j\}$ and $\{d_k^j\}$. Let us first derive a recursion relationship similar to (2.39) and (2.40) for the orthonormal shell expansion. From (3.44), (3.45), (3.42), and (3.43), we obtain

$$\hat{S}^j(\xi) = \hat{s}^0(\xi)\ 2^{j/2} \prod_{l=1}^{j} |m_0(2^{l-1}\xi)|^2, \tag{3.46}$$

$$\hat{D}^j(\xi) = \hat{s}^0(\xi)\ 2^{j/2} |m_1(2^{j-1}\xi)|^2 \prod_{l=1}^{j-1} |m_0(2^{l-1}\xi)|^2. \tag{3.47}$$

On defining the functions

$$m_0^j(\xi) = \prod_{l=1}^{j} m_0(2^{l-1}\xi), \tag{3.48}$$

so that

$$m_1^j(\xi) = m_1(2^{j-1}\xi) m_0^{j-1}(\xi), \tag{3.49}$$

we obtain from (2.39), (2.40) , (3.46), and (3.47)

$$\hat{S}^j(\xi) = m_0^j(\xi)\hat{s}^j(\xi), \tag{3.50}$$

$$\hat{D}^j(\xi) = m_1^j(\xi)\hat{d}^j(\xi). \tag{3.51}$$

Thus, to compute the auto-correlation shell coefficients from the orthonormal shell coefficients, we have to evaluate

$$\hat{s}^j(\xi) = \frac{\overline{m_0^j(\xi)}}{|m_0^j(\xi)|^2}\hat{S}^j(\xi), \tag{3.52}$$

and

$$\hat{d}^j(\xi) = \frac{\overline{m_1^j(\xi)}}{|m_1^j(\xi)|^2}\hat{D}^j(\xi). \tag{3.53}$$

In general, such computation leads to an unstable algorithm due to zeros of the denominators. However, in our case, this procedure is stable and the division by $|m_0^j(\xi)|^2$ and $|m_1^j(\xi)|^2$ in (3.52) and (3.53) does not cause problems because the numerators are always zero when the denominators are zero (see Proposition 2 below).

We observe that transforming back and forth between the orthonormal shell representation and the auto-correlation shell representation is done on each scale separately.

Properties of the auto-correlation shell

Let us define the following norm for the auto-correlation shell expansion:

$$\|f\|_{\mathcal{A}}^2 = \sum_{j=1}^{n_0} 2^{-j} \sum_{k=0}^{N-1} (D_k^j)^2 + 2^{-n_0} \sum_{k=0}^{N-1} (S_k^{n_0})^2, \tag{3.54}$$

where the coefficients D_k^j and $S_k^{n_0}$ are defined in (3.37) and (3.36). The norm (3.54) may be compared with the norm for the orthonormal shell (2.23). As for the orthonormal shell, the factor 2^{-j} in (3.54) is used to offset the redundancy of this representation. We now obtain the following estimate:

Proposition 2

$$\frac{1}{n_0+1}\|f\|^2 \le \|f\|_{\mathcal{A}}^2 \le \|f\|^2, \tag{3.55}$$

where $\|f\|$ is the L^2 norm of the vector f in $\mathbf{V}_0$ defined in (2.19).

This inequality guarantees that there exists a stable reconstruction algorithm from the auto-correlation shell coefficients. If the number of dyadic scales $n_0 \to \infty$, then the lower bound in (3.55) approaches zero and the reconstruction algorithm becomes unstable. In feasible practical applications, however, the number of dyadic scales does not exceed a small constant (e.g. $n_0 \le 50$), and the estimate (3.55) is sufficient for a stable reconstruction. It also shows that our construction is limited to finite dimensional subspaces.

Proof of Proposition 2. From (2.26) we have

$$\|f\|^2 = \|f\|_{\mathcal{S}}^2 = \sum_{j=1}^{n_0} 2^{-j} \sum_{k=0}^{N-1} (d_k^j)^2 + 2^{-n_0} \sum_{k=0}^{N-1} (s_k^{n_0})^2. \tag{3.56}$$

Using Parseval's equality, we have the following Fourier domain expressions:

$$\sum_{k=0}^{N-1} (s_k^j)^2 = \frac{1}{N} \sum_{k=0}^{N-1} |\hat{s}_k^j|^2, \tag{3.57}$$

and

$$\sum_{k=0}^{N-1} (d_k^j)^2 = \frac{1}{N} \sum_{k=0}^{N-1} |\hat{d}_k^j|^2. \tag{3.58}$$

Using the expressions (2.39),(2.40),(3.48), and (3.49), we rewrite (3.56) as

$$\|f\|_{\mathcal{S}}^2 = \frac{1}{N} \left[\sum_{j=1}^{n_0} \sum_{k=0}^{N-1} |\hat{s}_k^0|^2 \ |m_1^j(\xi_k)|^2 + \sum_{k=0}^{N-1} |\hat{s}_k^0|^2 \ |m_0^{n_0}(\xi_k)|^2 \right], \tag{3.59}$$

where $\xi_k = 2\pi k/N$. Similarly, for the norm of the auto-correlation shell expansion (3.54), we have

$$\|f\|_{\mathcal{A}}^2 = \sum_{j=1}^{n_0} 2^{-j} \sum_{k=0}^{N-1} (D_k^j)^2 + 2^{-n_0} \sum_{k=0}^{N-1} (S_k^{n_0})^2. \tag{3.60}$$

With the same arguments, the Fourier domain expression of (3.60) becomes

$$\|f\|_{\mathcal{A}}^2 = \frac{1}{N} \left[\sum_{j=1}^{n_0} \sum_{k=0}^{N-1} |\hat{s}_k^0|^2 \ |m_1^j(\xi_k)|^4 + \sum_{k=0}^{N-1} |\hat{s}_k^0|^2 \ |m_0^{n_0}(\xi_k)|^4 \right]. \tag{3.61}$$

Since

$$\sup_{0 \le \xi \le 2\pi} |m_0^j(\xi)|^2 \le 1 \quad \text{and} \quad \sup_{0 \le \xi \le 2\pi} |m_1^j(\xi)|^2 \le 1, \tag{3.62}$$

we immediately have from (3.61)

$$\|f\|_{\mathcal{A}}^2 \le \|f\|_{\mathcal{S}}^2. \tag{3.63}$$

As for the rest of the inequality of (3.55), using the Schwarz inequality in (3.59) we have

$$\begin{aligned}
\|f\|_{\mathcal{S}}^2 &\le \frac{1}{N} \left[\sum_{j=1}^{n_0} \left(\sum_{k=0}^{N-1} |\hat{s}_k^0|^2 \right)^{\frac{1}{2}} \left(\sum_{k=0}^{N-1} |\hat{s}_k^0|^2 \ |m_1^j(\xi_k)|^4 \right)^{\frac{1}{2}} + \left(\sum_{k=0}^{N-1} |\hat{s}_k^0|^2 \right)^{\frac{1}{2}} \left(\sum_{k=0}^{N-1} |\hat{s}_k^0|^2 \ |m_0^{n_0}(\xi_k)|^4 \right)^{\frac{1}{2}} \right] \\
&= \frac{\|f\|}{\sqrt{N}} \left[\sum_{j=1}^{n_0} \left(\sum_{k=0}^{N-1} |\hat{s}_k^0|^2 \ |m_1^j(\xi_k)|^4 \right)^{1/2} + \left(\sum_{k=0}^{N-1} |\hat{s}_k^0|^2 \ |m_0^{n_0}(\xi_k)|^4 \right)^{1/2} \right] \\
&\le \sqrt{n_0+1} \ \frac{\|f\|}{\sqrt{N}} \left(\sum_{j=1}^{n_0} \sum_{k=0}^{N-1} |\hat{s}_k^0|^2 \ |m_1^j(\xi_k)|^4 + \sum_{k=0}^{N-1} |\hat{s}_k^0|^2 \ |m_0^{n_0}(\xi_k)|^4 \right)^{1/2} \\
&= \sqrt{n_0+1} \ \|f\| \ \|f\|_{\mathcal{A}}.
\end{aligned} \tag{3.64}$$

Since $\|f\| = \|f\|_{\mathcal{S}}$ (see (2.26)), we obtain (3.55).

The following proposition (which is similar to Proposition 1) is essential in our approach to the reconstruction of signals from zero-crossings.

Proposition 3 *For any function $f \in \mathbf{V}_0$, $f(x) = \sum_{k=0}^{N-1} s_k^0 \varphi(x-k)$, the coefficients $\{S_k^j\}$ and $\{D_k^j\}$ defined in (3.36) and (3.37) satisfy the following identities*

$$\sum_{k=0}^{N-1} S_k^j \widetilde{\Phi}_{0,k} = \sum_{k=0}^{N-1} s_k^0 \widetilde{\Phi}_{j,k} \tag{3.65}$$

and

$$\sum_{k=0}^{N-1} D_k^j \widetilde{\Phi}_{0,k} = \sum_{k=0}^{N-1} s_k^0 \widetilde{\Psi}_{j,k}, \tag{3.66}$$

where $\widetilde{\Phi}_{0,k}(x) = \Phi_{0,k}(x)$, and $\widetilde{\Phi}_{j,k}$ and $\widetilde{\Psi}_{j,k}$ are defined in (3.27) and (3.26).

Proof. By taking the Fourier transform of the left hand side of (3.65) and using (3.46), we have

$$\hat{S}^j(\xi)\hat{\Phi}(\xi) = \hat{s}^0(\xi)\ 2^{j/2} \prod_{l=1}^{j} |m_0(2^{l-1}\xi)|^2\ \hat{\Phi}(\xi) = \hat{s}^0(\xi)\ 2^{j/2}\hat{\Phi}(2^j\xi), \tag{3.67}$$

where we have used the identity

$$\hat{\Phi}(\xi) = \prod_{l=1}^{\infty} |m_0(2^{-l}\xi)|^2. \tag{3.68}$$

The inverse Fourier transform of (3.67) yields (3.65). The relation (3.66) may be derived similarly.

Examples of the auto-correlation shell expansion

Let us illustrate the auto-correlation shell expansion using several examples. In Figure 5 we show the expansion of the unit impulse and its shifted version in the auto-correlation shell to illustrate the symmetry, smoothness, and shift invariance of this representation (see Figure 2 for comparison). In Figure 6 we display an example of a one-dimensional profile of an image. The auto-correlation shell coefficients of the signal in Figure 6 are shown in Figure 7. Figure 8 shows the corresponding average coefficients. In this case, we have used the auto-correlation functions of the Daubechies's wavelet with two vanishing moments and $L = 4$.

C. A direct reconstruction of signals from the auto-correlation shell coefficients

As we have shown in the previous subsection, the original signal may be reconstructed from the auto-correlation shell coefficients by converting them to the orthonormal shell coefficients followed by the reconstruction algorithm (2.44). Let us now construct an algorithm for reconstructing the original signal directly from the auto-correlation shell coefficients. Rewriting (3.44) and (3.45) and using the coefficients $\{a_k\}$ of (3.13), we have

$$S_k^j = \frac{1}{\sqrt{2}} \left[S_k^{j-1} + \frac{1}{2} \sum_{l=1}^{L/2} a_{2l-1} \left(S_{k+2^{j-1}(2l-1)}^{j-1} + S_{k-2^{j-1}(2l-1)}^{j-1} \right) \right], \tag{3.69}$$

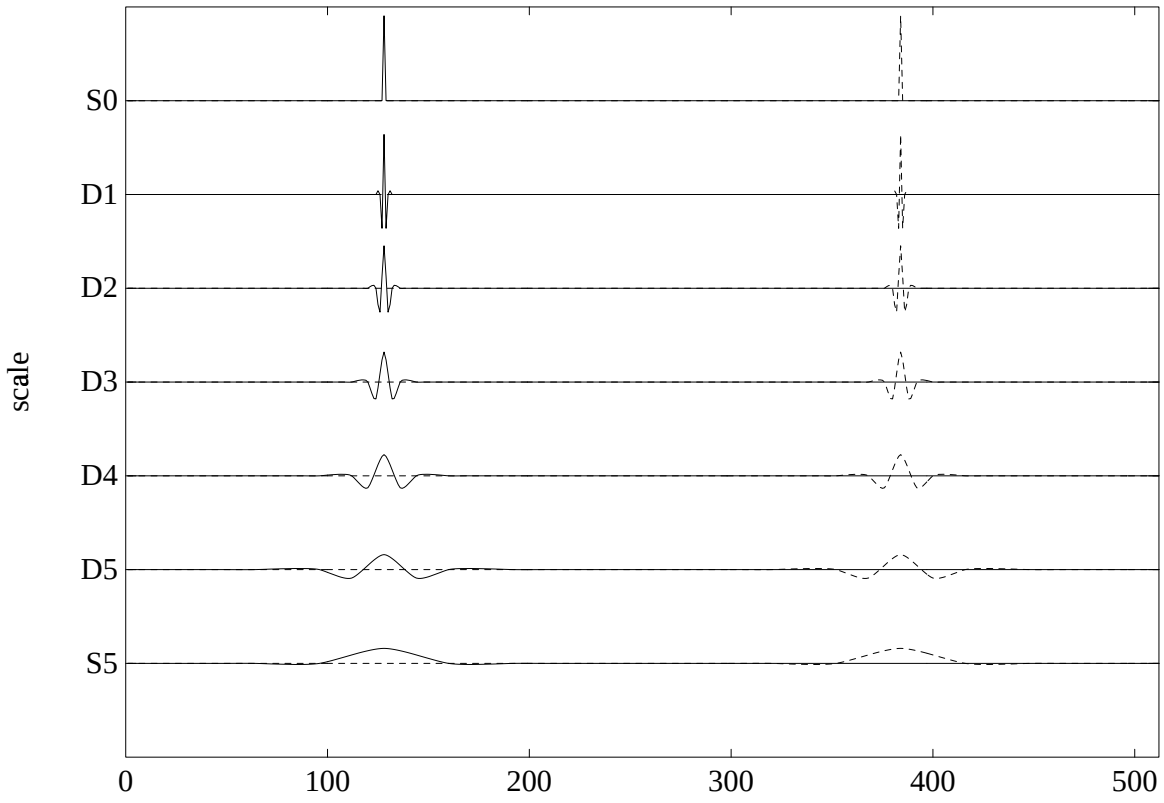

Figure 5: The expansion of two unit impulses in the auto-correlation shell using the auto-correlation functions of the Daubechies's wavelet with $L = 2M = 4$.

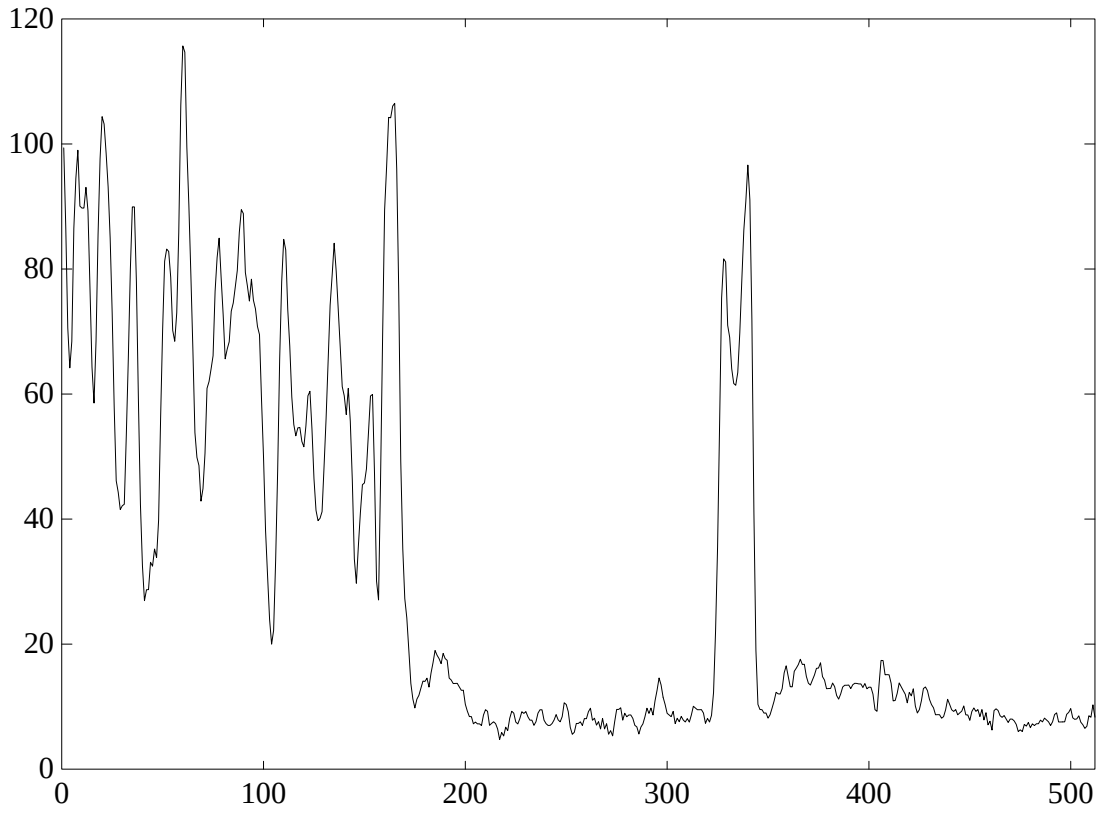

Figure 6: An example of a one-dimensional profile of an image.

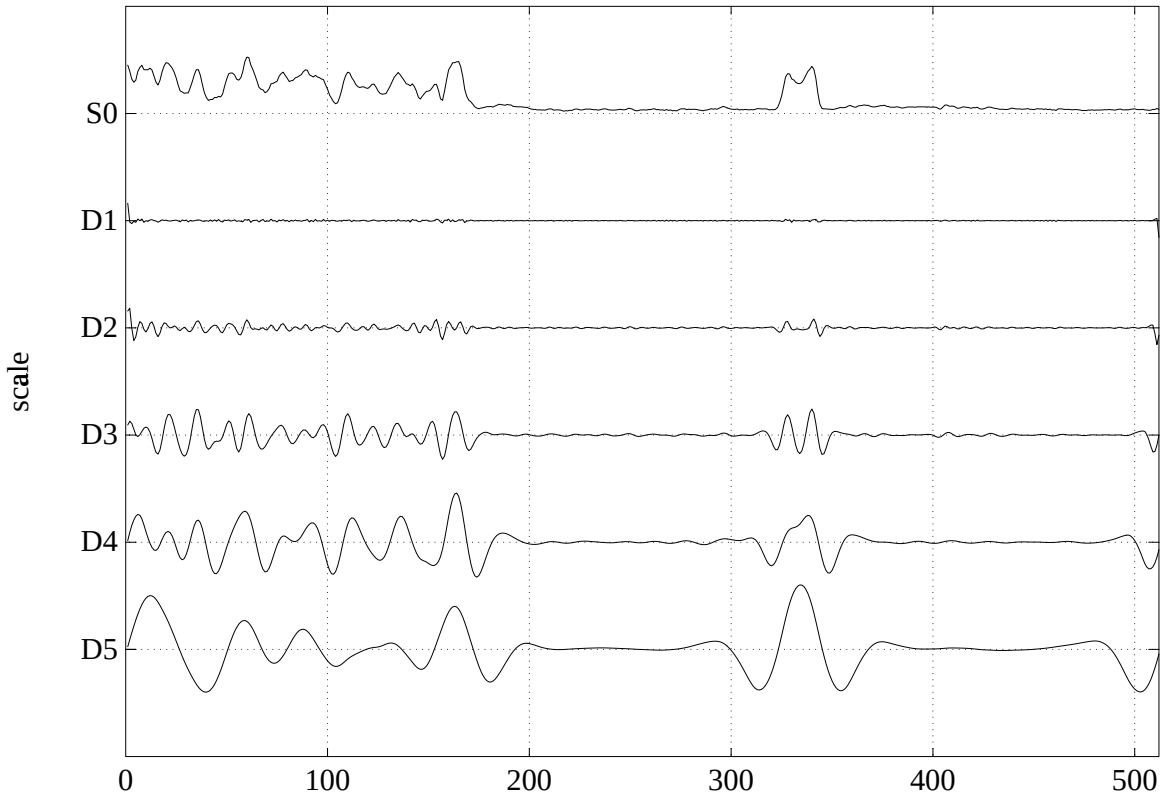

Figure 7: The expansion of the signal in the auto-correlation shell using the auto-correlation functions of the Daubechies's wavelet with $L = 2M = 4$. The top row is the original signal. Note that the locations of edges in the original signal correspond to the zero-crossings in this representation.

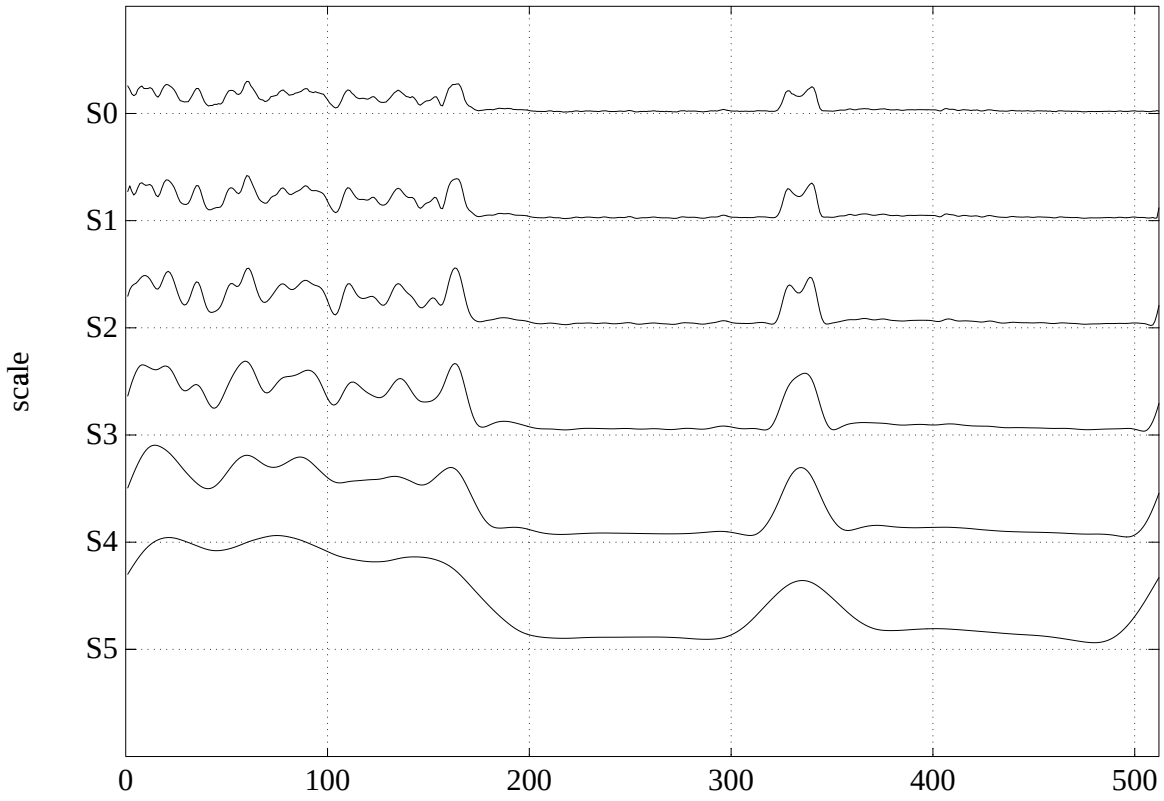

Figure 8: The averages on different scales (the top row is the original signal).

$$D_k^j = \frac{1}{\sqrt{2}} \left[S_k^{j-1} - \frac{1}{2} \sum_{l=1}^{L/2} a_{2l-1} \left(S_{k+2^{j-1}(2l-1)}^{j-1} + S_{k-2^{j-1}(2l-1)}^{j-1} \right) \right], \tag{3.70}$$

for $j = 1, \ldots, n_0,\ k = 0, \ldots, N-1$. By adding (3.69) and (3.70), we obtain a simple reconstruction formula,

$$S_k^{j-1} = \frac{1}{\sqrt{2}} \left(S_k^j + D_k^j \right), \tag{3.71}$$

for $j = 1, \ldots, n_0,\ k = 0, \ldots, N-1$. Given the auto-correlation shell coefficients $\{D_k^j\}_{1 \le j \le n_0,\ 0 \le k \le N-1}$ and $\{S_k^{n_0}\}_{0 \le k \le N-1}$, (3.71) leads to

$$s_k^0 = 2^{-n_0/2} S_k^{n_0} + \sum_{j=1}^{n_0} 2^{-j/2} D_k^j, \tag{3.72}$$

for $k = 0, \ldots, N-1$.

Like the orthonormal shell coefficients, $\{S_k^j\}$ and $\{D_k^j\}$ are redundant. This may be used to reconstruct a signal from subsampled auto-correlation shell coefficients.

D. The subsampled auto-correlation shell of compactly supported wavelets

We now turn to a question of reconstructing the original vector from a subsampled sequence of the auto-correlation shell coefficients. We demonstrate that it is possible to reconstruct the original signal if we keep a single additional number at each scale of the auto-correlation shell expansion, i.e., the Nyquist frequency components of the auto-correlation shell coefficients.

Let us define the *subsampled auto-correlation shell expansion* of a vector $f \in \mathbf{V}_0$ as follows.

$$\left\{ \sum_{k=0}^{2^{n-j}-1} d_k^j \Psi_{j,k}(x) \right\}_{1 \le j \le n_0} \quad \text{and} \quad \sum_{k=0}^{2^{n-n_0}-1} s_k^{n_0} \Phi_{n_0,k}(x), \tag{3.73}$$

where $\Phi_{j,k}$ and $\Psi_{j,k}$ are defined by

$$\Phi_{j,k}(x) = 2^{-j/2} \Phi(2^{-j}x - k), \tag{3.74}$$

$$\Psi_{j,k}(x) = 2^{-j/2} \Psi(2^{-j}x - k), \tag{3.75}$$

and the coefficients s_k^j and d_k^j are defined as the subsamples of the auto-correlation shell coefficients S_k^j and D_k^j as

$$s_k^j = S_{2^j k}^j, \tag{3.76}$$

and

$$d_k^j = D_{2^j k}^j \tag{3.77}$$

for $k = 0, 1, \ldots, 2^{n-j} - 1$. The notation s_k^j and d_k^j is local to this subsection (not to be confused with the one for the orthonormal wavelets).

The decomposition algorithm is similar to that for the orthonormal wavelets, and we compute

$$s_k^j = \sum_{l=-L+1}^{L-1} p_l s_{2k+l}^{j-1}, \tag{3.78}$$

and

$$d_k^j = \sum_{l=-L+1}^{L-1} q_l s_{2k+l}^{j-1}, \tag{3.79}$$

for $j = 1, \ldots, n_0,\ k = 0, \ldots, 2^{n-j} - 1$.

For the reconstruction, we first rewrite (3.78) and (3.79) in terms of the coefficients $\{a_k\}$ as

$$s_k^j = \frac{1}{\sqrt{2}} \left[s_{2k}^{j-1} + \frac{1}{2} \sum_{l=1}^{L/2} a_{2l-1} \left(s_{2k-2l+1}^{j-1} + s_{2k+2l-1}^{j-1} \right) \right], \tag{3.80}$$

$$d_k^j = \frac{1}{\sqrt{2}} \left[s_{2k}^{j-1} - \frac{1}{2} \sum_{l=1}^{L/2} a_{2l-1} \left(s_{2k-2l+1}^{j-1} + s_{2k+2l-1}^{j-1} \right) \right]. \tag{3.81}$$

By adding these two expressions, we obtain the coefficients of the $(j-1)$-th scale with even indices,

$$s_{2k}^{j-1} = \frac{1}{\sqrt{2}} \left(s_k^j + d_k^j \right), \tag{3.82}$$

for $j = 1, \ldots, n_0,\ k = 0, \ldots, 2^{n-j} - 1$. As for the coefficients with odd indices, we first define the sequence,

$$\begin{aligned} \Delta_k^j &= \frac{1}{\sqrt{2}} \left(s_k^j - d_k^j \right) && (3.83) \\ &= \frac{1}{2} \sum_{l=1}^{L/2} a_{2l-1} \left(s_{2k-2l+1}^{j-1} + s_{2k+2l-1}^{j-1} \right). && (3.84) \end{aligned}$$

By taking the Fourier transform of (3.83), we have

$$\begin{aligned} \hat{\Delta}^j(\xi) &= \sum_{k=0}^{2^{n-j}-1} \Delta_k^j \mathrm{e}^{\mathrm{i}k\xi} && (3.85) \\ &= \frac{1}{2} \sum_{k=0}^{2^{n-j}-1} \sum_{l=1}^{L/2} a_{2l-1} \left(s_{2k+2l-1}^{j-1} \mathrm{e}^{\mathrm{i}k\xi} + s_{2k-2l+1}^{j-1} \mathrm{e}^{\mathrm{i}k\xi} \right) && (3.86) \\ &= \hat{s}_{odd}^{j-1}(\xi/2) \sum_{l=1}^{L/2} a_{2l-1} \cos((2l-1)\xi/2), && (3.87) \end{aligned}$$

where

$$\hat{s}_{odd}^{j-1}(\xi/2) = \sum_{k=0}^{2^{n-j}-1} s_{2k+1}^{j-1} \mathrm{e}^{\mathrm{i}(2k+1)\xi/2}. \tag{3.88}$$

The division by $\sum_{l=1}^{L/2} a_{2l-1} \cos((2l-1)\xi/2)$ is not defined at the Nyquist frequency at $\xi = \pi$. For the uniqueness of the reconstruction, we compute the Nyquist frequency component at each scale and store it as a part of the decomposition algorithm. We then supply these data at the

reconstruction stage. The Nyquist frequency component of odd samples at the $(j-1)$-th scale may be simply computed as

$$\sigma_{Nyq}^{j-1} = \hat{s}_{odd}^{j-1}(\pi/2) = \mathrm{i} \sum_{k=0}^{2^{n-j}-1} (-1)^k s_{2k+1}^{j-1}. \tag{3.89}$$

In summary, the coefficients with odd indices can be recovered as the inverse Fourier transform of the following quantity:

$$\hat{s}_{odd}^{j-1}(\xi/2) = \begin{cases} \dfrac{\hat{\Delta}^j(\xi)}{\sum_{l=1}^{L/2} a_{2l-1} \cos((2l-1)\xi/2)} & \text{for } 0 \le \xi < \pi, \\ \sigma_{Nyq}^{j-1} & \text{for } \xi = \pi. \end{cases} \tag{3.90}$$

Remark 3 In [30] Burt referred to the multiresolution representations which have the same number of coefficients at each scale as the "full density pyramid." He referred to the multiresolution representations where the number of coefficients is reduced logarithmically as the "standard density pyramid." Burt also referred to the "double density pyramid," where the number of coefficients at each scale is twice that of the standard density pyramid, as the one often used in practice for image processing applications. If we double the number of coefficients on each scale in the subsampled auto-correlation shell expansion, then there is no need to keep the Nyquist frequency component at each scale.

IV A Review of Dubuc's Iterative Interpolation Scheme

The representation using the auto-correlation functions of compactly supported wavelets has a natural interpolation algorithm associated with it. This interpolation scheme is due to Dubuc [1] and has been extended in [2] by Deslauriers and Dubuc. This interpolation scheme may be arrived at by considering the auto-correlation function of the scaling function $\varphi(x)$ (see also [9]). Namely, for every wavelet (not necessarily compactly supported), the auto-correlation function $\Phi(x)$ of the scaling function $\varphi(x)$, gives rise to a symmetric iterative interpolation scheme and the auto-correlation function $\Phi(x)$ is exactly the "fundamental function" $F(x)$ introduced in [1], [2]. In particular, the Daubechies's wavelet with the quadrature mirror filters of length $L = 4$ and of two vanishing moments yields the scheme in [1]. And the general case of Daubechies's wavelets with M vanishing moments ($L = 2M$) leads to the iterative interpolation scheme using the Lagrange polynomials of degree $2M$ [2]. Examples of schemes other than the Lagrange iterative interpolation may be obtained using compactly supported wavelets other than those explicitly described in [5] (see e.g., [28], [6]).

This interpolation scheme allows us to use a natural algorithm for computing zero-crossings and slopes at the zero-crossings in the auto-correlation shell expansion in an efficient manner and with the prescribed accuracy.

Dubuc in [1] and Deslauriers and Dubuc in [2] considered the following problem: if B_n is the set of dyadic rationals $m/2^n, m = 0, 1, \ldots$, and the values of $f(x)$ are already given on the set B_0, then how may one extend f to $B_1, B_2, \ldots$ in an iterative manner so that the limit of this interpolation yields a uniformly continuous function?

Let $h = 1/2^{n+1}$ be a unit interval in the set B_{n+1}. For $x \in B_{n+1} \setminus B_n$, Dubuc have suggested the following formula to compute the value $f(x)$,

$$f(x) = \frac{9}{16}\left(f(x-h) + f(x+h)\right) - \frac{1}{16}\left(f(x-3h) + f(x+3h)\right). \tag{4.1}$$

Figure 9 illustrates a few steps of this iterative process applied to the unit impulse.

Deslauriers and Dubuc generalized this interpolation scheme as follows:

$$f(x) = \sum_{k \in \mathbf{Z}} F(k/2) f(x + kh), \quad \text{for} \quad x \in B_{n+1} \setminus B_n \text{ and } h = 1/2^{n+1}, \tag{4.2}$$

where the coefficients $F(k/2)$ are computed by generating the function satisfying

$$F(x/2) = \sum_{k \in \mathbf{Z}} F(k/2) F(x - k). \tag{4.3}$$

By comparing (4.2) and (4.3), we observe that the function $F(x)$ is an interpolation of the unit impulse $\{\delta_{0k}\}_{k \in \mathbf{Z}}$. Using this fact, the equation (4.2) may be rewritten as

$$f(x) = \sum_{k \in \mathbf{Z}} f(k) F(x - k) \qquad \text{for} \quad x \in \mathbf{R}. \tag{4.4}$$

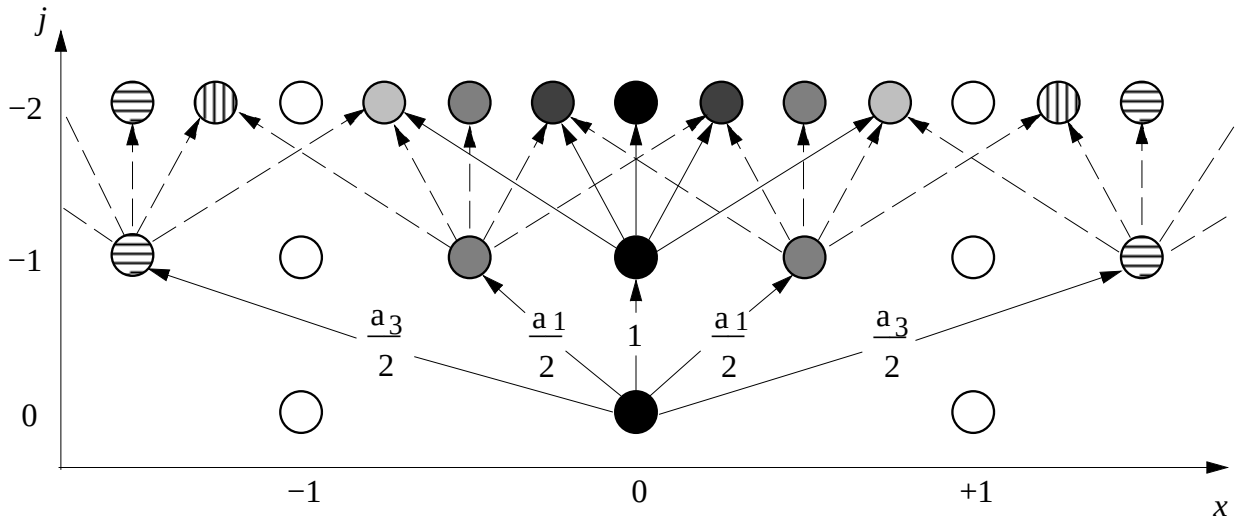

Figure 9: The Lagrange iterative interpolation of the unit impulse sequence with the associated quadrature mirror filter of length $L = 4$, i.e., $a_1 = 9/8$ and $a_3 = -1/8$. Black nodes at $x = 0$ indicate 1 and white nodes at $x = \pm 1$ have value 0. Shaded nodes have values other than 0 or 1. Note that the values of nodes existing at the j-th scale do not change at the $(j-1)$-th scale and higher. The result of repeating this procedure converges to $\Phi(x)$ as $j \to -\infty$.

In particular, they discussed an example connected with the Lagrange polynomial with $L = 2M$ nodes,

$$f(x) = \sum_{k=-M+1}^{M} \mathcal{P}_{2k-1}^{L}(0)\ f(x + (2k-1)h) \tag{4.5}$$

$$= \sum_{k=1}^{M} \mathcal{P}_{2k-1}^{L}(0)\ \left(f(x - (2k-1)h) + f(x + (2k-1)h)\right), \tag{4.6}$$

where $\{\mathcal{P}_{2k-1}^{L}(x)\}_{-M+1 \le k \le M}$ is a set of the Lagrange polynomials of the degree $L-1$ with nodes $\{-L+1, -L+3, \ldots, L-3, L-1\}$,

$$\mathcal{P}_{2k-1}^{L}(x) = \prod_{l=-M+1, l \neq k}^{M} \frac{x - (2l-1)}{(2k-1) - (2l-1)}. \tag{4.7}$$

In this case, the equation (4.3) reduces to

$$F_L(x) = F_L(2x) + \sum_{k=1}^{M} \mathcal{P}_{2k-1}^{L}(0)\ \left(F_L(2x - 2k + 1) + F_L(2x + 2k - 1)\right), \tag{4.8}$$

where F_L is the fundamental function of Dubuc and Deslauriers. This special case of (4.2) or (4.4) is called the "Lagrange iterative interpolation." The original Dubuc's scheme (4.1) corresponds to $L = 4$ in the scheme (4.5).

For general wavelets, we have the following proposition:

Proposition 4

$$F(x) = \Phi(x), \tag{4.9}$$

where $F(x)$ is the fundamental function defined in (4.3) and $\Phi(x)$ is the auto-correlation function of the scaling function $\varphi(x)$.

Proof. Let us compute the quantity $\Phi(k/2)$ using the two-scale difference equation (3.15)

$$\Phi(k/2) = \Phi(k) + \frac{1}{2}\sum_{l\in\mathbf{N}} a_{2l-1}\left(\Phi(k-2l+1) + \Phi(k+2l-1)\right). \tag{4.10}$$

Using the property (3.3), we have from (4.10)

$$\Phi(k/2) = a_k/2. \tag{4.11}$$

In other words, the two-scale difference equation for the function Φ in (3.15) may be rewritten as

$$\Phi(x/2) = \sum_{k\in\mathbf{Z}} \Phi(k/2)\Phi(x-k). \tag{4.12}$$

Equivalence of (4.3) and (4.12) combined with the uniqueness of the nontrivial L^1-solution to these equations (Theorem 2.1 of [31]) implies (4.9).

The vanishing moments of $\Phi(x)$ (see (3.18) and (3.19)) and Proposition 4 yield

Proposition 5 ([2]) *For any polynomial P of degree smaller than L, the Lagrange iterative interpolation of the sequence $f(n) = P(n)$, $n \in \mathbf{Z}$ via (4.5), is precisely the function $f(x) = P(x)$ for any $x \in \mathbf{R}$.*

The regularity of the fundamental function $F(x)$ may also be derived from the results of Daubechies and Lagarias[31]. To compute the derivative of the interpolated function, we differentiate (4.4):

Proposition 6 *If $h = 2^{-n}$, and if $x \in B_m$, where $m \le n$, then the derivative of an interpolation function $f(x)$ is computed via*

$$f'(x) = \sum_{k=1}^{L-2} r_k\left(f(x+kh) - f(x-kh)\right), \tag{4.13}$$

where

$$r_k = \int_{-\infty}^{+\infty} \varphi(x-k)\frac{d}{dx}\varphi(x)dx. \tag{4.14}$$

Note that the coefficients r_k coincide with those derived in [23] for the representation of the derivative operator in the orthonormal wavelet basis and may be computed using

Proposition 7 ([23]) *1. If the integral in (4.14) exists, then the coefficients $\{r_k\}_{k\in\mathbf{Z}}$ in (4.14) satisfy the following system of linear algebraic equations*

$$r_k = 2\left[r_{2k} + \tfrac{1}{2}\sum_{l=1}^{L/2} a_{2l-1}(r_{2k-2l+1} + r_{2k+2l-1})\right], \tag{4.15}$$

and

$$\sum_{k\in\mathbf{Z}} k\, r_k = -1, \tag{4.16}$$

where the coefficients a_{2l-1} are given in (3.13).

2. If the number of vanishing moments of the wavelet $M \geq 2$, then equations (4.15) and (4.16) have a unique solution with a finite number of non-zero r_k, namely, $r_k \neq 0$ for $-L+2 \leq k \leq L-2$ and

$$r_k = -r_{-k}. \tag{4.17}$$

We use the auto-correlation functions $\Phi(x), \Psi(x)$ and their derivatives $\Phi'(x), \Psi'(x)$ in the algorithm for reconstructing signals from the zero-crossings which we will discuss in the next section. Let us describe the algorithm for evaluating functions $\Phi(x)$ and $\Phi'(x)$ at any given point $x \in \mathbf{R}$ for any given accuracy. We use the iterative interpolation scheme to zoom in the interval around x until we reach the interval $[x-\epsilon, x+\epsilon]$, where ϵ is the prescribed accuracy. Once in this interval, the derivative at the center of this interval is computed using (4.13). The evaluation of the functions $\Psi(x)$ and $\Psi'(x)$ may be obtained from the formula (3.21), i.e., $\Psi(x) = 2\Phi(2x) - \Phi(x)$.

Using this algorithm, we computed $\Phi(x)$ and $\Phi'(x)$ which are shown in Figure 10. The same Figure may be obtained if we directly apply the iterative interpolation scheme to the unit impulse (see Figure 9; see also Dubuc [1] and Daubechies & Lagarias [31]).

Remark 4 The interpolation scheme discussed in this section "fills the gap" between the following two extreme cases:

If the number of vanishing moments $M = 1$ and the length of the quadrature mirror filter $L = 2$, then $\{\psi_{j,k}(x)\}$ is the Haar basis and we have

$$\Phi_{\text{Haar}}(x) = \begin{cases} 1+x & \text{for } -1 \leq x \leq 0, \\ 1-x & \text{for } 0 \leq x \leq 1, \\ 0 & \text{otherwise.} \end{cases} \tag{4.18}$$

The interpolation process is exactly *linear* interpolation. (The auto-correlation function of the characteristic function Φ_{Haar} is often called the *hat* function.)

Let us now consider the case where $M \to \infty$. Using the expressions (3.49)–(3.52) of [23], the relation (3.12) for the 2π periodic function $|m_0(\xi)|^2$ may be rewritten in terms of M as follows:

$$\begin{aligned} |m_0(\xi)|^2 &= \frac{1}{2} + \frac{1}{2}\sum_{k=1}^{M} a_{2k-1}\cos(2k-1)\xi \\ &= \frac{1}{2} + \frac{1}{2}C_M \sum_{k=1}^{M} \frac{(-1)^{k-1}\cos(2k-1)\xi}{(2k-1)\ (M-m)!\ (M+k-1)!}, \end{aligned} \tag{4.19}$$

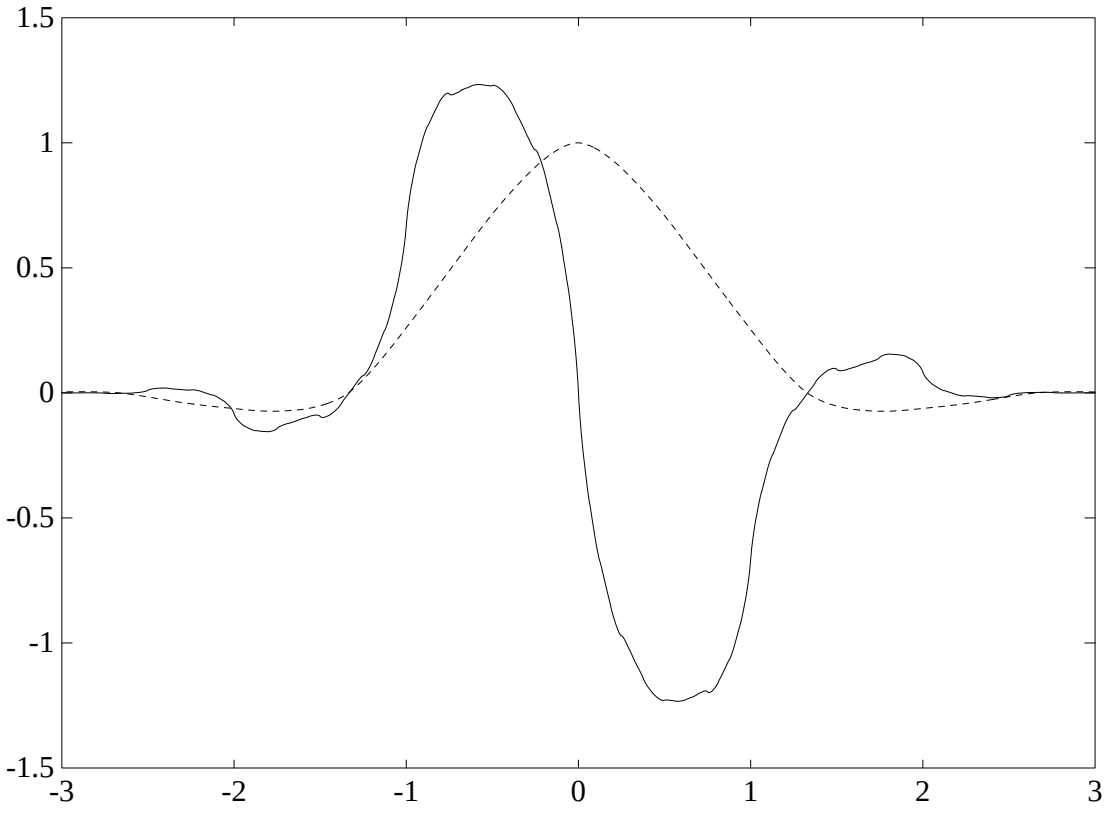

Figure 10: The auto-correlation function $\Phi(x)$ (dashed line) and its derivative $\Phi'(x)$ (solid line) with $L = 4$. Note the rough shape of $\Phi'(x)$.

where

$$C_M = \left[\frac{(2M-1)!}{(M-1)!\ 4^{M-1}} \right]^2. \tag{4.20}$$

If $M \to \infty$, then

$$|m_0(\xi)|^2 \to \frac{1}{2} + \frac{1}{2} \sum_{k=1}^{\infty} \frac{(-1)^{k-1}}{2k-1} \cos(2k-1)\xi, \tag{4.21}$$

which is exactly the Fourier coefficient of the characteristic function $\chi_{[-\pi/2,\pi/2]}(\xi)$. This implies that the corresponding auto-correlation function is

$$\Phi_\infty(x) = \mathrm{sinc}(x) = \frac{\sin \pi x}{\pi x}. \tag{4.22}$$

The interpolation process then corresponds to the so-called *band-limited* interpolation. Daubechies [6] noticed that if the number M of the vanishing moments of the compactly supported wavelet $\psi(x)$ approaches infinity, then the corresponding scaling function $\varphi(x)$ itself also approaches

$$\varphi_\infty(x) = \mathrm{sinc}(x). \tag{4.23}$$

As a result, we have the following relation,

$$\varphi_\infty(x) = \Phi_\infty(x), \tag{4.24}$$

and

$$\sqrt{2} h_k = \frac{a_k}{2} = \frac{\sin \pi k/2}{\pi k/2} \quad \text{for} \quad k \in \mathbf{Z}. \tag{4.25}$$

The auto-correlation function Φ of the wavelet corresponding to the quadrature mirror filter with M vanishing moments always satisfies the two-scale difference equation

$$\Phi(x/2) = \sum_{k=-M}^{M} \Phi(k/2)\Phi(x-k), \tag{4.26}$$

and (4.18) and (4.22) may be considered as the two extreme examples. Thus, the quadrature mirror filters with M vanishing moments, where $1 \le M < \infty$, provide a parameterized family of the symmetric iterative interpolation schemes.

V On Reconstructing Signals from Zero-Crossings

In this section, we formulate the problem of reconstructing signals from zero-crossings (and slopes at these points) in the auto-correlation shell. The outline of our approach is as follows: we compute and record the zero-crossings (and slopes at these zero-crossings) on each scale of the auto-correlation shell expansion within the prescribed numerical accuracy using the Dubuc's iterative interpolation scheme.

For reconstruction, we set up a system of linear algebraic equations, where the unknown vector is the original signal itself and the entries of the matrix are computed from the values of the auto-correlation function and its derivative at the integer translates of the zero-crossings. The signal is reconstructed by solving this linear system.

Reconstructing a signal from its zero-crossings by solving a linear system of equations has been proposed by S. Curtis and A. Oppenheim [32]. Their method requires a solution of a linear system where the unknowns are the Fourier coefficients and, therefore, the linear system is dense. It also requires multiple threshold-crossings rather than zero-crossings, and moreover, the quality of the reconstruction strongly depends on the choice of the thresholds.

We would like to note that in our approach we take advantage of multiresolution properties of the auto-correlation shell and, specifically, of Proposition 3. This proposition allows us to set the linear system directly for the unknown signal rather than the coefficients of its expansion. We note that this proposition does not hold if we were to use the scale-space filtering with Gaussians, for example.

If we were to use biorthogonal wavelet bases, then it is possible to set up a linear system similar to that constructed in this paper. In this case the difficulty is in keeping both the difference and average coefficients sufficiently smooth and balance this requirement with the computational efficiency. However, in this paper we limit ourselves to considering only the auto-correlation shell.

Zero-crossing detection and computation of slopes

Using the iterative interpolation scheme described in the previous section, we locate the zero-crossing locations of the set of functions $\{\sum_{k=0}^{N-1} D_k^j \Phi(x-k)\}_{1\le j\le n_0}$ within the prescribed numerical accuracy (in our examples we compute in double precision with $\epsilon = 10^{-14}$).

To compute the locations of zero-crossings, we recursively subdivide the unit interval bracketing the zero-crossing until the length of the subdivided interval bracketing that zero-crossing becomes less than the accuracy ϵ. The iterative interpolation scheme allows us to zoom in as much as we want around the zero-crossing. This process requires at most $O(-L\log_2\epsilon)$ operations per zero-crossing. Once the zero-crossing is found, the computation of the slope is merely the convolution of the $2(L-2)$ points around the zero-crossing with the filter coefficients $\{r_l\}_{1\le l\le L-2}$ in (4.13).

Reconstruction from zero-crossings

We address the following problem:

Given the coarsest subsampled average coefficients $\{S_{2^{n_0}k}^{n_0}\}_{0\le k\le 2^{n-n_0}-1}$, *and the zero-crossings and the slopes at these zero-crossings* $\{x_m^j, v_m^j\}_{1\le j\le n_0,\ 0\le m\le N_z^j-1}$, *where* N_z^j *is the number of zero-crossings of the function* $\sum_{k=0}^{N-1} D_k^j\Phi(x-k)$, *reconstruct the original vector* $\{s_k^0\}_{0\le k\le N-1}$.

Proposition 3 in Section III provides a simple mechanism for defining a linear system which relates the unknown signal $\{s_k^0\}$ and the values of the function Φ and its derivative at the integer translates of zero-crossings. Using the auto-correlation shell expansion of the signal, we immediately find the following relationships at all zero-crossings.

$$\sum_{k=0}^{N-1} D_k^j \Phi(x_m^j - k) = 0, \tag{5.1}$$

$$\sum_{k=0}^{N-1} D_k^j \Phi'(x_m^j - k) = v_m^j, \tag{5.2}$$

where $1 \le j \le n_0,\ 0 \le m \le N_z^j - 1$.

Applying Proposition 3 to (5.1) and (5.2), we have

$$\sum_{k=0}^{N-1} s_k^0 \widetilde{\Psi}_{j,k}(x_m^j) = 0, \tag{5.3}$$

$$\sum_{k=0}^{N-1} s_k^0\ 2^{-j} \widetilde{\Psi}'_{j,k}(x_m^j) = v_m^j. \tag{5.4}$$

Since it is easy to evaluate $\widetilde{\Psi}_{j,k}(x)$ and $\widetilde{\Psi}'_{j,k}(x)$ for any $x \in \mathbf{R}$ within the prescribed accuracy as described in the previous section, we interpret (5.3) and (5.4) as a system of linear algebraic equations where the original signal $\{s_k^0\}$ itself is the unknown vector.

Using the same proposition for the available average coefficients, we have

$$\sum_{k=0}^{N-1} s_k^0 \widetilde{\Phi}_{n_0,k}(x) = \sum_{k=0}^{N-1} S_k^{n_0} \Phi_{0,k}(x). \tag{5.5}$$

If we evaluate (5.5) at the integer point $x = 2^{n_0} l$, then we have

$$\sum_{k=0}^{N-1} s_k^0 \widetilde{\Phi}_{n_0,k}(2^{n_0} l) = S_{2^{n_0} l}^{n_0}, \tag{5.6}$$

for $l = 0, 1, \ldots, N_s - 1$, where $N_s = 2^{n-n_0}$.

We rewrite (5.3),(5.4), and (5.6) in a vector-matrix form as

$$\mathbf{A}\ \mathbf{s} = \mathbf{v}, \tag{5.7}$$

where $\mathbf{s} \in \mathbf{R}^N$ is a shorthand notation of the original signal $\{s_k^0\}$, and $\mathbf{v} \in \mathbf{R}^{2N_z + N_s}$ is a data vector

$$(0, v_0^1, \ldots, 0, v_{N_z^1 - 1}^1, \ldots\ldots, 0, v_0^{n_0}, \ldots, 0, v_{N_z^{n_0} - 1}^{n_0}, S_0^{n_0}, S_{2^{n_0}}^{n_0}, \ldots, S_{N-2^{n_0}}^{n_0})^T, \tag{5.8}$$

and finally, $\mathbf{A}$ is a $(2N_z + N_s) \times N$ matrix and has the following structure:

$$\mathbf{A} = \begin{pmatrix} \mathbf{A}^1 \\ \mathbf{A}^2 \\ \vdots \\ \mathbf{A}^{n_0} \\ \mathbf{S}^{n_0} \end{pmatrix}, \tag{5.9}$$

where $\mathbf{A}^j$ is a $2N_z^j \times N$ submatrix whose entries are

$$(\mathbf{A}^j)_{2k,l} = \widetilde{\Psi}_{j,l}(x_k^j), \tag{5.10}$$

$$(\mathbf{A}^j)_{2k+1,l} = 2^{-j}\widetilde{\Psi}'_{j,l}(x_k^j), \tag{5.11}$$

for $k = 0, \ldots, N_z^j - 1$ and $l = 0, \ldots, N-1$ and

$\mathbf{S}^{n_0}$ is a $N_s \times N$ submatrix where

$$(\mathbf{S}^{n_0})_{k,l} = \widetilde{\Phi}_{n_0,l}(2^{n_0}k), \tag{5.12}$$

for $k = 0, \ldots, N_s$ and $l = 0, \ldots, N-1$. (Note that we use vector and matrix indices starting from 0 rather than 1.) We note that the k-th row of the matrix $\mathbf{S}^{n_0}$ comprises the average coefficients at the scale n_0 of the auto-correlation shell expansion of the shifted unit impulse $\{\delta_{2^{n_0}k,l}\}_{0 \le l \le N-1}$.

Since the auto-correlation function $\widetilde{\Psi}_{j,k}(x)$ is compactly supported, the matrix $\mathbf{A}$ is sparse by construction. It is easy to check that the support of the function $\widetilde{\Psi}_{j,k}(x)$ is $2^{j+1}(L-1)$. Thus, the number $N_{\mathbf{A}}$ of non-zero entries of the matrix $\mathbf{A}$ is as follows:

$$N_{\mathbf{A}} = \sum_{j=1}^{n_0} 2N_z^j \; 2^{j+1}(L-1) + N_s \; 2^{n_0+1}(L-1) = 2(L-1)\left[\sum_{j=1}^{n_0} 2^j \; 2N_z^j + N\right]. \tag{5.13}$$

The number of zero-crossings usually decreases as the scale j increases. As a result, the number of the non-zero entries of the matrix $\mathbf{A}$ is essentially $O(N)$. The sparsity of this matrix may be used to solve the system (5.7) efficiently.

Whether we can solve the linear system (5.7) depends on the condition number of the matrix (5.9), which is affected by the distribution of locations of zero-crossings.

If there are very few zero-crossings (which means that the signal is zero over a significant part of its support) as, for example, in the expansion of the unit impulse $\{s_k^0 = \delta_{k_0,k}\}$ with only $2L$ zero-crossings at each scale, then we need to use additional constraints for solving the linear system (5.7). There might be several approaches to introduce these additional constraints. One approach (which might be sufficient in some applications) would be to consider the generalized inverse of (5.9). Another possible approach (that we have experimented with), is to introduce a heuristic constraint that the distance between the adjacent zero-crossings at the j-th scale does not exceed $2^{j+1}(L-1)$.

To impose these constraints on the solution of the system of linear equations (5.7), we rewrite (5.7) in terms of the difference coefficients $\{D_k^j\}$ as follows:

$$\mathbf{L}\ \mathbf{d} = \mathbf{v}, \tag{5.14}$$

where $\mathbf{d} \in \mathbf{R}^{Nn_0+N_s}$ is a vector of the auto-correlation shell coefficients including the subsampled coarsest averages, i.e.,

$$(D_0^1, \ldots, D_{N-1}^1, \ldots\ldots, D_0^{n_0}, \ldots, D_{N-1}^{n_0}, S_0^{n_0}, S_{2^{n_0}}^{n_0}, \ldots, S_{N-2^{n_0}}^{n_0})^T, \tag{5.15}$$

and $\mathbf{L}$ is a $(2N_z + N_s) \times (Nn_0 + N_s)$ matrix,

$$\begin{pmatrix} \mathbf{L}^1 & \mathbf{0} & \cdots & \cdots & \mathbf{0} \\ \mathbf{0} & \mathbf{L}^2 & \cdots & \cdots & \vdots \\ \vdots & & \ddots & & \vdots \\ \vdots & \cdots & \cdots & \mathbf{L}^{n_0} & \mathbf{0} \\ \mathbf{0} & \cdots & \cdots & \mathbf{0} & \mathbf{I}_{N_s} \end{pmatrix}, \tag{5.16}$$

where $\mathbf{I}_{N_s}$ is the N_s dimensional identity matrix, and $\mathbf{L}^j$ is a $2N_z^j \times N$ block matrix whose entries are

$$L^j_{2k,l} = \Phi(x^j_k - l), \tag{5.17}$$

$$L^j_{2k+1,l} = \Phi'(x^j_k - l), \tag{5.18}$$

for $k = 0, \ldots, N_z^j - 1$ and $l = 0, \ldots, N - 1$. The relation between the vector $\mathbf{d}$ and the original signal $\mathbf{s}$ is described as follows:

$$\mathbf{d} = \mathbf{T}\ \mathbf{s}, \tag{5.19}$$

where the matrix $\mathbf{T}$ is a transformation matrix from $\mathbf{s}$ to $\mathbf{d}$,

$$\mathbf{T} = \begin{pmatrix} \mathbf{Q}_1 \\ \mathbf{Q}_2\mathbf{P}_1 \\ \mathbf{Q}_3\mathbf{P}_2\mathbf{P}_1 \\ \vdots \\ \mathbf{Q}_{n_0}\mathbf{P}_{n_0-1}\cdots\mathbf{P}_1 \\ [\mathbf{P}_{n_0}\mathbf{P}_{n_0-1}\cdots\mathbf{P}_1]^{n_0} \end{pmatrix}, \tag{5.20}$$

where $[\mathbf{P}]^{n_0}$ is a collection of the row vectors of P whose indices are $0, 2^{n_0}, \ldots, N - 2^{n_0}$ and the matrices $\mathbf{P}_j, \mathbf{Q}_j$ are defined as shorthand notation for the pyramid algorithm (3.44) and (3.45) as follows:

$$S^j = \mathbf{P}_j S^{j-1}, \tag{5.21}$$

$$D^j = \mathbf{Q}_j S^{j-1}, \tag{5.22}$$

where S^j and D^j are N dimensional vectors representing the j-th scale coefficients $\{S^j_k\}_{0 \le k \le N-1}$ and $\{D^j_k\}_{0 \le k \le N-1}$. Using the matrix $\mathbf{T}$, the matrix $\mathbf{A}$ may be obtained from $\mathbf{L}$ by

$$\mathbf{A} = \mathbf{L}\ \mathbf{T}. \tag{5.23}$$

We now impose a constraint that if there are $2^{j+1}(L-1)$ or more consecutive null columns in the submatrix $\mathbf{L}^j$, then the corresponding coefficients must be zero. These constraints may be written as

$$\mathbf{C}\ \mathbf{d} = \mathbf{0}, \tag{5.24}$$

and $\mathbf{C}$ is an $(Nn_0 + N_s)$ dimensional square matrix of the form

$$\begin{pmatrix} \mathbf{C}^1 & \mathbf{0} & \cdots & \cdots & \mathbf{0} \\ \mathbf{0} & \mathbf{C}^2 & \cdots & \cdots & \vdots \\ \vdots & & \ddots & & \vdots \\ \vdots & \cdots & \cdots & \mathbf{C}^{n_0} & \mathbf{0} \\ \mathbf{0} & \cdots & \cdots & \mathbf{0} & \mathbf{0} \end{pmatrix}, \tag{5.25}$$

where the submatrix $\mathbf{C}^j$ is a N dimensional diagonal matrix as

$$(\mathbf{C}^j)_{k,k} = \begin{cases} 1 & \text{if } D_k^j \text{ must be zero,} \\ 0 & \text{otherwise.} \end{cases} \tag{5.26}$$

To eliminate $\mathbf{d}$ in favor of $\mathbf{s}$ in equation (5.24), we use the transformation matrix $\mathbf{T}$, and define the matrix $\mathbf{B} \in \mathbf{R}^{(2N_z+N_s)\times N}$,

$$\mathbf{B} = \mathbf{C}\ \mathbf{T}. \tag{5.27}$$

The problem may now be stated as follows:

$$\textit{Minimize} \quad \|\mathbf{A}\ \mathbf{s} - \mathbf{v}\| \quad \textit{subject to} \quad \|\mathbf{B}\ \mathbf{s}\| = 0. \tag{5.28}$$

Using the method of Lagrange multipliers, we obtain the least square solution

$$\hat{\mathbf{s}} = (\mathbf{A}^T\mathbf{A} + \lambda\mathbf{B}^T\mathbf{B})^{-1}\mathbf{A}^T\mathbf{v}. \tag{5.29}$$

Since we consider minimizing $\|\mathbf{A}\ \mathbf{s} - \mathbf{v}\|$ and satisfying $\|\mathbf{B}\ \mathbf{s}\| = 0$ equally important, we assume $\lambda = 1$.

Note that our formulation is completely linear except for the process of the zero-crossing detection.

Reconstruction examples

Example 1: We first use the signal shown in the Figure 6 in Section III as an example. In this case, the size of the matrix $\mathbf{A}$ is 1852 by 512. The relative L^2 error of the reconstructed signal compared with the original signal (see Figure 6) is 5.674436×10^{-13}. The accuracy threshold ϵ was set to 10^{-14} in this case.

Example 2: Let us consider the reconstruction of the unit impulse $\{\delta_{k_0,k}\}$ from its zero-crossings and slopes in the auto-correlation shell expansion. In this case, the size of the matrix $\mathbf{A}$ is 56×64. In Figure 11a we display the matrix $\mathbf{A}^T\mathbf{A}$ in (5.29). In Figure 11b we show the matrix with the constraints $\mathbf{A}^T\mathbf{A} + \mathbf{B}^T\mathbf{B}$. It is easy to see that the constraints serve to condition the linear system. The relative L^2 error with the constraints is 7.417360×10^{-15} whereas the error of the solution by the generalized inverse without the constraints is 3.247662×10^{-4}.

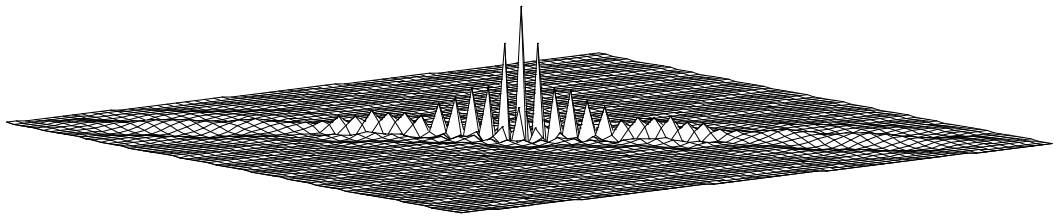

(a)

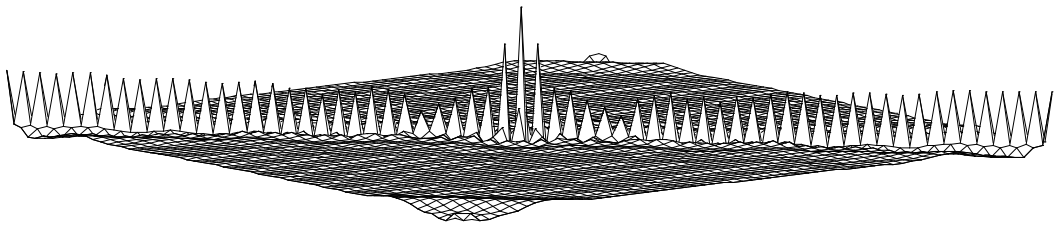

(b)

Figure 11: The effect of the constraints in the reconstruction of the unit impulse from zero-crossing and slopes. (a) The unconstrained matrix $\mathbf{A}^T\mathbf{A}$. (b) The constrained matrix $\mathbf{A}^T\mathbf{A} + \mathbf{B}^T\mathbf{B}$.

VI Conclusions

In this paper we have proposed the auto-correlation shell representation, a "hybrid" shift-invariant multiresolution representation using the auto-correlation functions of compactly supported wavelets. The auto-correlation functions of the corresponding scaling functions induce the symmetric iterative interpolation of Dubuc [1] and Deslauriers and Dubuc [2] which allows us to interpolate efficiently on all dyadic rationals. This property of the auto-correlation functions enables us to compute zero-crossings and slopes at the zero-crossings of the auto-correlation shell representation. This representation also gives us an explicit relation between the original signal and its expansion coefficients so that we can set up a system of linear algebraic equations for reconstructing the original signal from these zero-crossings and slopes. The original signal is reconstructed within prescribed numerical accuracy by solving this linear system.

References

[1] S. Dubuc, "Interpolation through an iterative scheme," *J. Math. Anal. and Appl.*, vol. 114, pp. 185–204, 1986.

[2] G. Deslauriers and S. Dubuc, "Symmetric iterative interpolation processes," *Constructive Approximation*, vol. 5, pp. 49–68, 1989.

[3] Y. Meyer, *Ondelettes et Opérateurs*. Paris: Hermann, 1990.

[4] R. Kronland-Martinet, J. Morlet, and A. Grossmann, "Analysis of sound patterns through wavelet transforms," *J. Pattern Recognition and Artifitial Intell.*, vol. 1, no. 2, 1987.

[5] I. Daubechies, "Orthonormal bases of compactly supported wavelets," *Comm. Pure and Appl. Math.*, vol. 41, pp. 909–996, 1988.

[6] I. Daubechies, "Orthonormal bases of compactly supported wavelets. II. variations on a theme," *preprint*, 1990.

[7] A. Cohen, I. Daubechies, and J.-C. Feauveau, "Biorthogonal bases of compactly supported wavelets," *preprint*, 1990.

[8] M. Vetterli and C. Herley, "Wavelets and filter banks: theory and design," technical report, Center for Telecommunications Research, Columbia University, 1990.

[9] M. J. Shensa, "The discrete wavelet transform: wedding the à trous and Mallat algorithms," *IEEE Trans. Signal Processing*, Oct. 1992. to appear.

[10] M. Holschneider, R. Kronland-Martinet, J. Morlet, and A. Grossmann, "A real-time algorithm for signal analysis with the help of the wavelet transform," in *Wavelets, Time-Frequency Methods and Phase Space* (J. M. Combes, A. Grossmann, and P. Tchamitchian, eds.), pp. 286–297, Springer-Verlag, 1989.

[11] P. Dutilleux, "An implementation of the "algorithme à trous" to compute the wavelet transform," in *Wavelets, Time-Frequency Methods and Phase Space* (J. M. Combes, A. Grossmann, and P. Tchamitchian, eds.), pp. 298–304, Springer-Verlag, 1989.

[12] N. E. Hurt, *Phase Retrieval and Zero Crossings*. Dordrecht, The Netherlands: Kluwer Academic Publishers, 1989.

[13] D. Marr, *Vision*. W.H.Freeman and Company, 1982.

[14] A. P. Witkin, "Scale space filtering," in *Proc. 8th Joint Conf. Artificial Intell.*, pp. 1019–1023, 1983.

[15] J. J. Koenderink, "The structure of images," *Biol. Cybern.*, vol. 50, pp. 363–370, 1984.

[16] A. L. Yuille and T. Poggio, "Fingerprints theorems for zero crossings," *J. Opt. Soc. Amer.*, vol. 2, pp. 683–692, May 1985.

[17] A. L. Yuille and T. Poggio, "Scaling theorems for zero crossings," *IEEE Trans. Pattern Anal. Machine Intell.*, vol. 8, pp. 15–25, Jan. 1986.

[18] R. A. Hummel, "Representation based on zero-crossings in scale-space," in *Proc. IEEE Conf. Comput. Vision, Pattern Recognition*, pp. 204–209, 1986.

[19] R. Hummel and R. Moniot, "Reconstruction from zero crossings in scale space," *IEEE Trans. Acoust., Speech, Signal Processing*, vol. 37, pp. 2111–2130, Dec. 1989.

[20] S. Mallat, "Zero-crossings of a wavelet transform," *IEEE Trans. Inform. Theory*, vol. 37, pp. 1019–1033, July 1991.

[21] S. Mallat and S. Zhong, "Complete signal representation with multiscale edges," Technical Report 483, Courant Institute of Mathematical Sciences, New York University, Dec. 1989.

[22] M. Duval-Destin, M. Muschietti, and B. Torresani, "Continuous wavelet decompositions, multiresolution and contrast analysis," *SIAM J. Math. Anal.*, 1992. to appear.

[23] G. Beylkin, "On the representation of operators in bases of compactly supported wavelets," *SIAM J. Numer. Anal.*, 1991. to appear.

[24] P. J. Burt, "Fast filter transforms for image processing," *Comput. Graphics and Image Processing*, vol. 16, pp. 20–51, 1981.

[25] P. J. Burt and E. H. Adelson, "The Laplacian pyramid as a compact image code," *IEEE Trans. Communications*, vol. 31, pp. 532–540, Apr. 1983.

[26] S. Mallat, "Multiresolution approximations and wavelet orthonormal bases in $\mathbf{L}^2(\mathbf{R})$," *Trans. Amer. Math. Soc.*, vol. 315, pp. 69–87, Sep. 1989.

[27] Y. Meyer, "Ondelettes et functions splines," technical report, séminaire EDP, Ecole Polytechnique, Paris, France, 1986.

[28] G. Beylkin, R. Coifman, and V. Rokhlin, "Fast wavelet transforms and numerical algorithms I," *Comm. Pure and Appl. Math.*, vol. 44, pp. 141–183, 1991.

[29] A. Grossmann, "Wavelet transforms and edge detection," in *Stochastic Processes in Physics and Engineering* (S. Albeverio, P. Blanchard, M. Hazewinkel, and L. Streit, eds.), pp. 149–157, D. Reidel Publishing Company, 1988.

[30] P. J. Burt, "Algorithms and architectures for smart sensing," in *Proc. Image Understanding Workshop*, pp. 139–153, Apr. 1988.

[31] I. Daubechies and J. C. Lagarias, "Two-scale difference equations, I. Global regularity of solutions & II. Local regularity, infinite products of matrices and fractals," *SIAM J. Math. Anal.*, 1991. to appear.

[32] S. R. Curtis and A. V. Oppenheim, "Reconstruction of multidimensional signals from zero crossings," *J. Opt. Soc. Am. A*, vol. 4, pp. 221–231, Jan. 1987.

List of things to do

*** Constraints for the delta function reconstructions. Distance between the neighboring zero-crossings must be a function of the scale. Is it really less than 2^j? (V)

*** Iterative reconstruction. Detect ZC with enforcing the spurious ZC's slopes to zero $\leftrightarrow$ Solve LS by GINV.

$\times$ The same scheme for zero-crossing works for biorthogonal system? (V)

** What happens if we use the coiflet for the Dubuc's scheme? This case is covered by the DD paper? (IV)

* Refer to some work of Coifman. (atomic decomposition) (III)

* Check the stability estimate for the subsampled ACS. (III)

** Further application: filtering based on the magnitudes of slopes. (V)

* Further considerations: Reconstruction in the scale-by-scale basis. Can we recover $\{D_k^j\}$ directly? (V)

* Future directions: 2D, link with wavelet-based linear solver, BCR, etc.